The deubiquitinating enzymes UBP12 and UBP13 negatively regulate the activity of the ubiquitin-dependent peptidases DA1, DAR1 and DAR2

Hannes Vanhaeren[1,2,3,4], Ying Chen[1,2], Mattias Vermeersch[1,2], Valerie De Vleeschhauwer[1,2], Geert Persiau[1,2], Dominique Eeckhout[1,2], Geert De Jaeger[1,2], Kris Gevaert[3,4], Dirk Inzé[1,2]*

[1]VIB Center for Plant Systems Biology, Technologiepark 71, 9052, Zwijnaarde, Belgium; [2]Department of Plant Biotechnology and Bioinformatics, Ghent University, Technologiepark, 71, 9052, Zwijnaarde, Belgium; [3]VIB Center for Medical Biotechnology, Albert Baertsoenkaai, 3, 9000, Ghent, Belgium; [4]Department of Biomolecular Medicine, Ghent University, Albert Baertsoenkaai 3, 9000, Ghent, Belgium

* For correspondence: dirk.inze@psb.vib-ugent.be

Abstract

Protein ubiquitination is a very diverse post-translational modification leading to protein degradation or delocalization, or altering protein activity. In *Arabidopsis thaliana*, two E3 ligases, BIG BROTHER (BB) and DA2, activate the latent peptidases DA1, DAR1 and DAR2 by mono-ubiquitination at multiple sites. Subsequently, these activated peptidases destabilize various positive regulators of growth. Here, we show that two ubiquitin-specific proteases, UBP12 and UBP13, deubiquitinate DA1, DAR1 and DAR2, hence reducing their peptidase activity. Overexpression of *UBP12* or *UBP13* strongly decreased leaf size and cell area, and resulted in lower ploidy levels. Mutants in which *UBP12* and *UBP13* were downregulated produced smaller leaves that contained fewer and smaller cells. Remarkably, neither UBP12 nor UBP13 were found to be cleavage substrates of the activated DA1. Our results therefore suggest that UBP12 and UBP13 work upstream of DA1, DAR1 and DAR2 to restrict their protease activity and hence fine-tune plant growth and development.

Introduction

Ubiquitination plays a prominent role in the signaling cascades of many plant hormones (Santner and Estelle, 2010), such as auxins (Salehin et al., 2015), jasmonates (Nagels Durand et al., 2016), gibberellins (Wang and Deng, 2011), and strigolactones (Marzec, 2016), but also in many plant developmental processes and responses to stress (Shu and Yang, 2017). Therefore, a very tight control of this process and a high substrate specificity, which is mainly determined by the E3 ubiquitin ligases (Shu and Yang, 2017), are required. The tremendous diversity of the ubiquitination system and its potential in post-translational regulation are illustrated by the presence of more than 1400 genes that encode E3 ligases in Arabidopsis (Vierstra, 2009). Furthermore, there is a high diversity of ubiquitination types and combinations with other post-translational modifications (PTMs) (Callis, 2014; Swatek and Komander, 2016), as well as of the fate of the ubiquitinated protein, such as degradation, delocalization or changes in activity (Swatek and Komander, 2016).

In contrast to the more intensively studied action of E3 ligases, insights into the specific roles of deubiquitination enzymes (DUBs) in plant growth and development are only recently emerging. DUBs can generate free ubiquitin from tandem-linear repeats (Callis et al., 1995; Callis et al., 1990), are able to trim ubiquitin chains by hydrolyzing the isopeptide bond between ubiquitin molecules, and they can remove covalently bound ubiquitin from proteins (Komander et al., 2009). The Arabidopsis

41 genome codes for around 50 DUBs. As in yeast and mammals, they can be divided into five classes: the
42 ubiquitin C-terminal hydrolases (UHCs), JAB1/MPN/MOV34 (JAMM) domain DUBs that are zinc
43 metalloproteases, ovarian tumor proteases, the Machado-Josephin domain (MJD) DUBs, and the
44 ubiquitin binding proteins (UBPs), which is the largest group (Isono and Nagel, 2014). All UBPs contain
45 specific catalytic Cys- and His-boxes, which are highly conserved in both sequence and length (Zhou et
46 al., 2017). Based on their sequence homology and protein domain organization, these 27 members can
47 be further divided into 14 subfamilies (Yan et al., 2000). UBP12 and UBP13 are the largest UBPs and
48 contain a unique meprin and TRAF homology (MATH) domain. They were first reported to be functional
49 deubiquitinating enzymes that negatively regulate plant immunity (Ewan et al., 2011). Since then, both
50 proteins have been described to be involved in diverse molecular pathways. Mutations in *UBP12* and
51 *UBP13* result in early flowering and a decreased periodicity of circadian rhythm (Cui et al., 2013).
52 Molecularly, GIGANTEA (GI) recruits UBP12 and UBP13 to the ZEITLUPE (ZTL) photoreceptor complex,
53 which antagonizes the E3 ligase activity of ZTL and hereby stabilizes GI, ZTL and TOC1 [TIMING OF CAB
54 (CHLOROPHYLL A/B-BINDING PROTEIN EXPRESSION) 1] protein levels (Lee et al., 2019). In addition,
55 UBP12 and UBP13 can regulate the expression of several genes by deubiquitinating ubiquitinated H2A
56 (H2Aub) upon associating with LIKE HETEROCHROMATIN PROTEIN 1, a plant-specific polycomb group
57 (PcG) protein (Derkacheva et al., 2016). Polyubiquitination of MYC2 by the PUB10 E3 ligase can be
58 counteracted by UBP12 and UBP13, preventing degradation of MYC2 by the 26S proteasome which
59 then activates jasmonic acid signaling (Jeong et al., 2017). In a similar manner, ROOT GROWTH FACTOR
60 RECEPTOR 1 (RGFR1) and ORESARA 1 (ORE1) are deubiquitinated and therefore stabilized by UBP12
61 and UBP13, leading to an increased sensitivity of roots to the RGF1 peptide hormone (An et al., 2018)
62 and an acceleration in leaf senescence (Park et al., 2019), respectively.

63   Mutations in *UBP12* or *UBP13* decrease rosette leaf number and double mutants display
64 severe developmental defects (Cui et al., 2013). However, a direct link between these deubiquitinating
65 enzymes and leaf growth and development remained unclear. Here, we found that UBP12 and UBP13
66 interact with DA1, DAR1 and DAR2 *in vivo*. DA1, DAR1 and DAR2 have previously been documented to
67 negatively regulate leaf growth. Upon multiple mono-ubiquitination by BIG BROTHER (BB) or DA2,
68 these latent peptidases are activated to cleave growth regulators, such as UBP15, TCP14, TCP15 and
69 TCP22 (Dong et al., 2017). In addition, the activating E3 ligases BB and DA2 are cleaved and BB is
70 subsequently degraded by the N-degron pathway, mediated by PROTEOLYSIS 1 (PRT1) (Dong et al.,
71 2017). Single knock-outs in *DA1*, *DAR1* and *DAR2* only have very subtle effects on organ size (Dong et
72 al., 2017; Li et al., 2008). Plant growth is however strongly enhanced in the double mutant *da1ko_dar1-
73 1*, comparable to *da1-1* mutants, which carry a point mutation (DA1^{R358K}) (Li et al., 2008). The latter
74 mutation has a dominant-negative action towards DA1 and DAR1 (Li et al., 2008) and causes a
75 reduction in peptidase activity (Dong et al., 2017). Rosette growth is however severely impaired in the
76 triple mutant *da1ko_dar1-1_dar2-1* and the size of leaf cells and the extent of endoreduplication are
77 reduced (Peng et al., 2015). This phenotype can be complemented by ectopic expression of *DA1*, *DAR1*
78 or *DAR2*, suggesting they work redundantly in leaves (Peng et al., 2015). On the other hand,
79 overexpression of *GFP-DA1* results in smaller organs with fewer cells (Vanhaeren et al., 2017). Mutants
80 of *UBP15* can abolish the *da1-1* phenotype and give rise to smaller organs (Du et al., 2014). Inversely,
81 ectopic expression of *UBP15* enhances growth (Du et al., 2014; Liu et al., 2008).

82   Here, we demonstrate that UBP12 and UBP13 not only bind DA1, DAR1 and DAR2, but can also
83 remove ubiquitin from these proteins, rendering them in an inactive state. Moreover, UBP12 and
84 UBP13 were not found to be proteolytically cleaved by DA1, DAR1 or DAR2, indicating they work
85 upstream in this pathway. In line with these findings, *UBP12* and *UBP13* mutants and overexpression

86   lines exhibit overlapping macroscopic, cellular and molecular phenotypes as *35S::GFP-DA1*
87   overexpression lines and *da1ko_dar1-1_dar2-1* mutants, respectively. Our data provide evidence for
88   a pivotal role of UBP12 and UBP13 in restricting the protease activity od DA1, DAR1 and DAR2 during
89   plant growth and development.

Results

DA1, DAR1 and DAR2 interact with UBP12 and UBP13 *in vivo*

92   Genetic modifier screens previously identified several interactors of DA1 that either activate its
93   peptidase activity or are subjected to proteolytic cleavage by DA1. To gain further insights into the DA1
94   growth-regulatory pathway, we generated Arabidopsis lines that overexpressed GFP-tagged fusion
95   proteins of DA1, DAR1 and DAR2. Total protein extracts were isolated from eight-day-old seedlings and
96   incubated with anti-GFP beads to purify the bait proteins and their interactors. Label free
97   quantification identified a significant enrichment (p-value < 0.01) of the UBIQUITIN-SPECIFIC
98   PROTEASE 12 (UBP12) and UBP13 in the GFP-DA1 and GFP-DAR1 samples (Figure 1A-B) among other
99   interaction candidates (Figure 1–figure supplement 1, Figure 1-source data 1). Despite the much lower
100   levels of DAR2 MS/MS counts and a lower DAR2 bait protein coverage (Figure 1–figure supplement 2-
101   3), we found a significant enrichment of UBP12 at a less stringent threshold (p-value < 0.05) and UBP13
102   at the border of significance (Figure 1C, Figure 1-source data 1).
103   Next, we measured the expression levels of *DA1*, *DAR1*, *DAR2*, *UBP12* and *UBP13* in isolated
104   wild-type (Col-0) leaves in a detailed time-course from leaf primordium initiation to maturity. Both
105   *UBP12* and *UBP13* are highly and evenly expressed throughout leaf development at comparable levels
106   (Figure 1–figure supplement 4). Also *DA1*, *DAR1* and *DAR2* are expressed during leaf development as
107   demonstrated before (Peng et al., 2015), albeit *DAR2* at a lower level (Figure 1–figure supplement 4).
108   Taken together, *UBP12* and *UBP13* are co-expressed during leaf development and interact with DA1,
109   DAR1 and DAR2 *in vivo*.

Miss-expression of *UBP12* and *UBP13* alters leaf size

111   Because DA1, DAR1 and DAR2 are known to restrict plant organ growth, we examined the role of
112   UBP12 and UBP13 in regulating leaf size by generating several independent transgenic *35S::UBP12* and
113   *35S::UBP13* lines. All overexpression lines showed a reduction in rosette area (Figure 2A). In addition,
114   leaves were more round than those of the Col-0, a phenotype which can also be observed in *da1-1*
115   plants, and the petioles were found to be shorter. For several *35S::UBP13* lines, we were unable to
116   produce stable seed stocks because the homozygous plants were stunted in growth (Figure 2A) and
117   failed to produce a flower stalk and seeds. We continued with two independent lines for further
118   phenotypic analysis: two homozygous *UBP12* lines (*35S::UBP12_3.1* and *35S::UBP12_3.2*) and two
119   *UBP13* lines from which heterozygous plants were selected (*35S::UBP13_1.1* and *35S::UBP13_2.3*)
120   (Figure 2A). These lines all had a significant increase in their respective transgene expression compared
121   to Col-0 (Figure 2–figure supplement 1).
122   In parallel, we screened two independent *UBP12* T-DNA insertion lines [*ubp12-1*
123   (GABI_244E11) and *ubp12-2* (GABI_742C10)] and three independent *UBP13* T-DNA lines [*ubp13-1*
124   (SALK_128312), *ubp13-2* (SALK_024054) and *ubp13-3* (SALK_132368)]. After leaf area measurements,
125   we could observe a decrease in leaf area in the *ubp12-2* mutants (Figure 2B), in which the levels of
126   both *UBP12* and *UBP13* transcripts were previously shown to be downregulated (Cui et al., 2013).
127   Mutant lines in which only the expression of either *UBP12* or *UBP13* was downregulated, displayed no
128   differences in leaf size compared to the control (Figure 2–figure supplement 2-5).

3

129   The final leaf size is determined by cell proliferation and cell expansion. To identify which of
130   these processes were affected in the *ubp12-2* mutant and in the *UBP12* and *UBP13* overexpression
131   lines, we performed a cellular analysis on the abaxial pavement cells of mature leaves. In all
132   overexpression lines, the significant decrease in leaf area (29%, 26%, 33% and 36% for *35S::UBP12_3.1*,
133   *35S::UBP12_3.2*, *35S::UBP13_1.1* and *35S::UBP13_2.3*, respectively) was caused by a strong reduction
134   in cell area (26%, 40%, 24% and 46% for *35S::UBP12_3.1*, *35S::UBP12_3.2*, *35S::UBP13_1.1* and
135   *35S::UBP13_2.3*, respectively), whereas the decrease in *ubp12-2* leaf size (32%) resulted from a
136   reduction in cell area (21%) and cell number (11%) (Figure 2C). Remarkably, besides a general decrease
137   in pavement cell area, we could observe a larger proportion of very small cells in the *UBP12* and *UBP13*
138   overexpression lines (Figure 2–figure supplement 6), which was even more pronounced in homozygous
139   *35S::UBP13_1.1* plants (Figure 2–figure supplement 7). A cell area distribution plot confirmed that
140   indeed all independent *UBP12* and *UBP13* overexpression lines harbored a larger proportion of these
141   small cells in addition to a general decrease in mature pavement cell size (Figure 2D). For the *ubp12-2*
142   mutant, no differences in cell area distribution compared to Col-0 could be observed (Figure 2–figure
143   supplement 8).

144   **Overexpression of *UBP12* or *UBP13* delays the onset of endoreduplication**

145   A strong reduction in cell size is often correlated with decreased levels of endoreduplication. To
146   explore this into more detail, we harvested a time-course of the first leaf pair of Col-0, *35S::UBP12_3.1*
147   and *35S::UBP13_2.3* (hereafter referred to as *35S::UBP12* and *35S::UBP13*) plants, spanning all major
148   developmental time points. At nine days after stratification (DAS), all leaf cells of the three lines
149   exhibited a 2C or 4C content, demonstrating the majority of cells are still in the mitotic cell cycle (Figure
150   3A). From 12 DAS onwards, cells with 8C started to appear, indicating the onset of endoreduplication.
151   At 12 DAS, leaves of *35S::UBP12* plants contained a significantly larger proportion of 2C cells (53%)
152   than those of the Col-0 (43%) and a significantly lower amount of 4C cells (44% and 52%, respectively).
153   At 15 DAS, the amount of 8C nuclei was significantly lower in *35S::UBP12* (28%) than in the control
154   (35%) (Figure 3A). Similar, but more pronounced observations were found in *35S::UBP13* leaves, in
155   which a significantly higher amount of 2C cells was detected at 12 DAS (61%) and 15 DAS (42%)
156   compared to Col-0 (43% and 25%, respectively). In addition, a lower level of 4C cells was found at 12
157   DAS (35% in *35S::UBP13*, 52% in Col-0) and fewer cells with 8C were present at 15, 18, 21 and 27 DAS
158   in *35S::UBP13* (22%, 33%, 35% and 35%, respectively) compared to Col-0 (35%, 42%, 42% and 46%,
159   respectively) (Figure 3A). An alternative way to illustrate endoreduplication levels is the
160   endoreduplication index, representing the average amount of endocycles a nucleus underwent.
161   Generally, slightly lower endoreduplication levels could be observed in *35S::UBP12* leaves (Figure 3–
162   figure supplement 1), whereas a stronger effect was clear in *35S::UBP13* leaves, with significant
163   differences at 12, 15 and 21 DAS (Figure 3–figure supplement 2).

164   Because the strongest effects were visible in the younger time points, we subsequently
165   prepared RNA from the younger third leaf until 18 DAS. Considering the higher 2C levels in *35S::UBP12*
166   and *35S::UBP13* (Figure 3A) and the presence of larger proportions of small cells in the leaf epidermis
167   at 21 DAS (Figure 2D, Figure 2–figure supplement 6-7), we measured the expression of several
168   transcriptional markers of cell proliferation that previously have been described to positively regulate
169   growth: *ANGUSTIFOLIA3* (*AN3*) (Horiguchi et al., 2005), *AINTEGUMENTA* (*ANT*), (Mizukami and Fischer,
170   2000), *GROWTH-REGULATING FACTOR 5* (*GRF5*) (Horiguchi et al., 2005; Vercruyssen et al., 2015), *KLUH*
171   *(Anastasiou et al., 2007)* and the cell division marker *CYCLINB1;1* (*CYCB1;1*) (Doerner et al., 1996; Shaul
172   et al., 1996). At 9 DAS, when all epidermal cells are actively dividing (Andriankaja et al., 2012), we could

4

173   observe a significantly higher expression of *ANT*, *GRF5* and *KLUH* in *35S::UBP13* lines compared to the
174   Col-0 (Figure 3B). Later in development at 12 DAS, a large portion of the Col-0 cells should have exited
175   the mitotic division cycle and start to differentiate (Andriankaja et al., 2012; Donnelly et al., 1999;
176   Kazama et al., 2010). Still, there was a significant higher expression of *AN3* and *GRF5* and the cell
177   division marker *CYCB1;1* in *35S::UBP13* leaves (Figure 3C). On 15 DAS, the expression levels of *ANT* and
178   *CYCB1;1* were elevated in *35S::UBP13* leaves (Figure 3–figure supplement 3) and finally, at 18 DAS, *ANT*
179   was still significantly higher expressed in *35S::UBP13* compared to the Col-0 (Figure 3–figure
180   supplement 4). These results indicate that especially during the early developmental stages of leaf
181   growth, endoreduplication and cell differentiation are delayed in *UBP12* an *UBP13* overexpression
182   lines.

183   UBP12 and UBP13 can deubiquitinate activated DA1, DAR1 and DAR2

184   The latent peptidases DA1, DAR1 and DAR2 can be activated upon ubiquitination by the E3 ligases BB
185   or DA2. Considering the enzymatic function of UBP12 and UBP13, they might counteract this by
186   deubiquitinating these activated peptidases. To test this, we performed an *in vitro* ubiquitination assay
187   to generate ubiquitinated DA1, DAR1 an DAR2, followed by a deubiquitination step with UBP12 or
188   UBP13, or their respective catalytic mutants, UBP12^{C208S} and UBP13^{C207S} (Cui et al., 2013; Ewan et al.,
189   2011). DA1, DAR1 and DAR2 were expressed and isolated as HIS-MBP fusion proteins and UBP12,
190   UBP13, UBP12^{C208S} and UBP13^{C207S} as GST fusion proteins. To mediate the ubiquitination, recombinant
191   HIS-DA2 was purified as the E3 ligase. The ubiquitinated peptidases were incubated with equal
192   amounts of either GST-UBP12, GST-UBP12^{C208S}, GST-UBP13 or GST-UBP13^{C207S}. Figure 4A shows that
193   ubiquitinated HIS-MBP-DA1 can be deubiquitinated by GST-UBP12 or GST-UBP13, but their respective
194   catalytic mutants fail to do so. Similar deubiquitination activities could be observed for the substrates
195   DAR1 and DAR2 (Figure 4B-C). Because the peptidase activity of DA1, DAR1 and DAR2 is similarly
196   activated upon ubiquitination and they function redundantly to regulate leaf size and ploidy, we chose
197   to focus on DA1 in our next experiments.

198   To demonstrate the specificity of UBP12 and UBP13, we performed additional
199   deubiquitination experiments with several UBPs from different subfamilies (Yan et al., 2000): GST-
200   UBP3, GST-UBP24 and GST-UBP15, of which the latter had already been demonstrated to function in
201   the same pathway of DA1 (Du et al., 2014) as its cleavage substrate (Dong et al., 2017). Ubiquitinated
202   HIS-MBP-DA1 was incubated with equal amounts of GST-UBP12, GST-UBP13, GST-UBP3, GST-UBP15
203   and GST-UBP24. We found again that both GST-UBP12 and GST-UBP13 could strongly deubiquitinate
204   HIS-MBP-DA1, but no such effect could be observed upon addition of GST-UBP3, GST-UBP15 or GST-
205   UBP24 (Figure 4D). These experiments demonstrate the deubiquitination specificity by UBP12 and
206   UBP13.

207   UBP12 and UBP13 are no substrates of the activated DA1

208   Our observation that UBP12 and UBP13 can deubiquitinate DA1, DAR1 and DAR2 suggests they work
209   upstream in this growth-regulatory pathway. Considering the peptidase activity of DA1, DAR1 and
210   DAR2, we tested whether these deubiquitinating enzymes could in their turn be substrates. For this
211   purpose, we incubated GST-UBP12, GST-UBP12^{C208S}, GST-UBP13 and GST-UBP13^{C207S} with
212   ubiquitinated HIS-MBP-DA1 or the peptidase-deficient HIS-MBP-DA1^{H418A,H422A} (Dong et al., 2017). The
213   catalytic UBP mutants were added to the assay because they are unable to deubiquitinate DA1 (Figure
214   4A) and, hence, are longer exposed to the activated peptidase. However, after 4 h of incubation, the
215   intensities of all GST-tagged UBP proteins were equal and no additional cleaving fragments could be

216   observed in the HIS-MBP-DA1 samples compared to those with HIS-MBP-DA1^{H418A,H422A} (Figure 5A).
217   Similar results were observed in the reactions in which the catalytic mutants of UBP12 or UBP13 were
218   incubated with ubiquitinated HIS-MBP-DA1 or HIS-MBP-DA1^{H418A,H422A} (Figure 5A).

219   Previously, it has been demonstrated that the dwarfed phenotype of strong *BB* overexpression
220   lines could largely be rescued by ectopic co-expression of *DA1*, as a result of cleavage and
221   destabilization of BB proteins (Dong et al., 2017). Similarly, we generated double overexpression lines
222   of *35S::GFP-DA1* and *35S::UBP12* or *35S::UBP13* (Figure 5–figure supplement 1). Compared to the Col-
223   0, leaf areas were reduced in *35S::GFP-DA1* (Figure 5B), as described before (Vanhaeren et al., 2017).
224   In all double overexpression lines, we could observe similar phenotypes as in the *35S::UBP12* and
225   *35S::UBP13* lines in the Col-0 background (Figure 2A), suggesting that the *UBP12* and *UBP13*
226   overexpression phenotype is dominant and UBP12 and UBP13 are not destabilized by DA1.

227   Thus, our biochemical, genetic and phenotypic analyses show that UBP12 and UBP13 are no cleavage
228   substrates, but act upstream of DA1, DAR1 and DAR2 to counteract their ubiquitination. By limiting
229   their peptidase activity, UBP12 and UBP13 fine-tune leaf growth, cell size and endoreduplication.

Discussion

231   Ubiquitination is an important post-transcriptional modification that comes in various forms of
232   complexity, which can lead to diverse effects on the fate of the substrate protein (Callis, 2014; Swatek
233   and Komander, 2016). The latent peptidases DA1, DAR1 and DAR2 are activated upon multiple mono-
234   ubiquitination by BB and DA2 and can subsequently cleave several growth regulators (Dong et al.,
235   2017). In this study, we identified two ubiquitin-specific proteases, UBP12 an UBP13, that interact with
236   DA1, DAR1 and DAR2 *in vivo*. Our experiments demonstrate that these UBPs work antagonistically to
237   BB and DA2. Incubation of ubiquitinated DA1, DAR1 or DAR2 with either UBP12 or UBP13 resulted in
238   strong deubiquitination. Similar experiments with other UBPs, such as UBP3, UBP15 and UBP24,
239   demonstrated that this activity was specific for UBP12 and UBP13. Interestingly, UBP15 has already
240   been shown to interact genetically with DA1 (Du et al., 2014) and can be cleaved by activated DA1
241   proteins (Dong et al., 2017). Our results indicate that UBP15 has no deubiquitination activity towards
242   DA1 and acts therefore downstream in this pathway. On the other hand, UBP12 and UBP13 are no
243   substrates of DA1 unlike UBP15 (Dong et al., 2017; Du et al., 2014), which suggests they work more
244   upstream in this signaling cascade. Most probably, UBP15 deubiquitinates and alters the fate of other
245   downstream growth-regulating proteins. UBP12 and UBP13 have recently been described to
246   deubiquitinate various poly-ubiquitinated proteins, preventing their proteasomal degradation (An et
247   al., 2018; Jeong et al., 2017; Lee et al., 2019; Park et al., 2019). In addition, they can decrease the levels
248   of mono-ubiquitinated H2A (Derkacheva et al., 2016) and remove multiple mono-ubiquitinations from
249   DA1, DAR1 and DAR2 as described here. This demonstrates the flexibility of these UBPs towards
250   different types of ubiquitination (Clague et al., 2019).

251   In contrast to the early flowering time-related genes (Cui et al., 2013), downregulation of either
252   *UBP12* or *UBP13* did not alter leaf size, indicating that these genes work redundantly in controlling leaf
253   size. The leaf area was only reduced in *ubp12-2* mutants, in which levels of both *UBP12* and *UBP13* are
254   decreased (Cui et al., 2013). The subsequently decreased deubiquitination activity towards DA1, DAR1
255   and DAR2 could result in an accumulation of the activated peptidases in *ubp12-2* mutants, leading to
256   a decrease in cell number and leaf area. A similar phenotype is also observed in *GFP-DA1*
257   overexpressing plants (Vanhaeren et al., 2017) and in the *ubp15* mutant (Du et al., 2014; Liu et al.,
258   2008). In contrast, high ectopic expression of either *UBP12* or *UBP13* would result in very low levels of

6

259 ubiquitinated DA1, DAR1 and DAR2, leading to a severe disturbance of leaf development. Indeed,
260 *35S::UBP12* and *35S::UBP13* plants were strongly reduced in growth in a similar manner as
261 *da1ko_dar1-1_dar2-1* triple mutants (Peng et al., 2015). A more detailed cellular and molecular
262 analysis of *35S::UBP12* and *35S::UBP13* leaves revealed more parallels, such as a strong reduction in
263 cell area and a decrease in ploidy levels at the early stages of leaf development, which were also
264 observed in *da1ko_dar1-1_dar2-1* plants (Peng et al., 2015). The complete absence of DA1, DAR1 and
265 DAR2 proteins in *da1ko_dar1-1_dar2-1* plants could however explain its stronger reduction in
266 endoreduplication than that of *UBP12* and *UBP13* overexpression lines, in which ubiquitination of DA1,
267 DAR1 and DAR2 can still occur, but is likely kept at a very low level. In addition, several markers of cell
268 proliferation were found to be more highly expressed in *35S::UBP12* and *35S::UBP13* during early
269 stages of leaf development, similarly as observed in plants that contain a DA1^{R358K} mutation
270 (Vanhaeren et al., 2017), which reduces the peptidase activity of DA1 (Dong et al., 2017). UBP12 and
271 UBP13 form thus an additional layer of post-translational regulation to fine-tune organ growth in the
272 growth-regulatory pathway of DA1, DAR1 and DAR2.
273 In wild-type conditions, a correct balance between inactive and active (ubiquitinated) DA1,
274 DAR1 and DAR2 results in an intact exit from mitosis in leaf cells and standard ploidy levels, which leads
275 to normal plant growth (Figure 6A). High levels of UBP12 or UBP13 can however shift the balance to
276 inactivated DA1, DAR1 and DAR2, which results in a delayed endoreduplication, a severe reduction in
277 cell size and stunted plant growth (Figure 6B). Low levels of UBP12 and UBP13 will on the other hand
278 lead to an increase in activated DA1, DAR1 and DAR2 levels and limit plant growth by reducing both
279 cell area and cell number (Figure 6C). A tight balance between active and inactive DA1, DAR1 and DAR2
280 is hence crucial for normal plant development. With *UBP12* and *UBP13* expression levels being
281 relatively constant throughout leaf development, unknown post-translational modifications of UBP12
282 and UBP13 are likely to alter the activity or specificity towards DA1, DAR1 and DAR2, as is the case with
283 other deubiquitinating enzymes (Huang and Cochran, 2013).

284 Over the years, it has become increasingly clear that DUBs play a greater role in the development of
285 eukaryotes than just processing and recycling free ubiquitin; many DUBs are involved in fine-tuning
286 molecular pathways by stabilizing proteins (An et al., 2018; Jeong et al., 2017; Lee et al., 2019; Park et
287 al., 2019), through controlling protein endocytosis (Crespo-Yàñez et al., 2018; Row et al., 2006), by
288 mediating DNA damage repair (Nijman et al., 2005) and by regulating transcription (Derkacheva et al.,
289 2016; Joo et al., 2007; Zhu et al., 2007) to name a few. Potentially, DUBs could remove ubiquitin of
290 existing chains so other chain types can be formed or other PTMs can be added.
291 Although our knowledge of organ growth has increased substantially over the last years, the
292 developmental triggers that initiate the ubiquitination of DA1, DAR1 and DAR2 by BB and DA2, the
293 dominant-negative nature of DA1^{R358K}, other potential substrates proteins of the ubiquitin-activated
294 peptidases and other post-translational regulatory elements remain some of the many compelling
295 mysteries on this intriguing growth-regulatory pathway.

Material and methods
Plant material and growth conditions
298 All *Arabidopsis thaliana* mutants and overexpression lines that were used in this study were from the
299 Col-0 background. *ubp12-1* (GABI_244E11), *ubp12-2* (GABI_742C10), *ubp13-1* (SALK_128312), *ubp13-2* (SALK_024054) and *ubp13-3* (SALK_132368) were kindly provided by Dr. Xia Cui (Chinese Academy
301 of Agricultural Sciences, Beijing, China). The respective T-DNA insertions were verified by PCR. The

302 *35S::GFP-DA1*, *35S::GFP-DAR1* and *35S::GFP-DAR2* lines were generated by Gateway cloning using the
303 pK7WGF2 destination vector, the *35S::UBP12* and *35S::UBP13* lines using the pFAST-G02. Because the
304 latter overexpression lines contained the *OLE1::GFP* construct (Shimada et al., 2010), we could select
305 positive seeds using a fluorescence binocular. The T-DNA lines were grown in soil for 25 days at 21°C
306 and 16-h day/8-h night cycles for the phenotyping experiments. All overexpression lines were grown
307 *in vitro* on plates containing half-strength Murashige and Skoog (MS) medium supplemented with 1%
308 sucrose with a density of one plant per 4 cm^2. These plants were grown for 21 days at 21°C and 16-h
309 day/8-h night cycles. Seedlings for the immunoprecipitation followed by tandem mass spectrometry
310 (IP-MS/MS) were grown for 8 DAS in liquid half-strength MS medium supplemented with 1% sucrose
311 under shaking conditions (100 rpm) at 21°C and 16-h day/8-h night cycles. For all experiments, the
312 seeds were stratified in the dark for 2 days at 4°C before being placed in the respective growth rooms.
313 Each quantitative experiment was performed in at least three independent biological repeats, meaning
314 they were sown and harvested at a different time. All genotyping and cloning primers that were used
315 in this study are listed in Supplementary Table 1.

316 **Leaf measurements and cellular analysis**

317 Leaves were dissected from the rosette and placed on a square plate containing 1% agar. The plants
318 were imaged and the leaf area was analyzed using ImageJ v1.45 (NIH; http://rsb.info.nih.gov/ij/). For
319 the cellular analysis, samples of leaf 3 (overexpression lines) and leaf 5 (*ubp12-2*) were cleared in 70%
320 ethanol and mounted in lactic acid on a microscope slide. The total leaf blade area was measured for
321 at least ten representative leaves under a dark-field binocular microscope. Abaxial epidermal cells at
322 the center of the leaf blade, avoiding major veins, were drawn with a microscope equipped with
323 differential interference contrast optics (DM LB with 403 and 633 objectives; Leica) and a drawing tube
324 for at least 3 leaves. Photographs of leaves and scanned cell drawings were used to measure leaf and
325 individual cell area, respectively, as described by Andriankaja et al. (2012). The statistical analysis of
326 the cellular data was performed in R 3.5.2 (www.r-project.org).

327 ***In vitro* deubiquitination and cleaving assays**

328 The coding sequences of UBP3, UBP12, UBP13, UBP15 and UBP24 were inserted in the pDEST15
329 (Thermofisher) destination vector using Gateway cloning to generate GST-UBP3, GST-UBP12, GST-
330 GST-UBP13, GST-UBP15 and GST-UBP24. The coding sequences of DA1, DAR1 and DAR2 were cloned
331 into pDEST-HIS-MBP using Gateway cloning to generate HIS-MBP-DA1, HIS-MBP-DAR1 and HIS-MBP-
332 DAR2. The HIS-DA2 (pET24a) construct was kindly provided by Dr. Michael Bevan (JIC, Norwich, UK).
333 To generate the respective catalytic mutants, we performed site-directed mutagenesis on the entry
334 clones of the respective genes by performing a PCR with primers containing the mutation. After the
335 PCR, 5 µl of Buffer B and 1 µl of DpnI (Promega) were added to each reaction. After an overnight
336 incubation, competent DH5α *E. coli* cells were transformed and the presence of the mutation was
337 checked by sequencing. All expression vectors were transformed into competent BL21 (DE3) *E. coli*
338 cells. For each protein, the optimal conditions to obtain sufficient soluble proteins were determined
339 (Supplementary Table 2). GST-tagged proteins were purified from the bacterial lysate with Glutathione
340 Sepharose 4B beads (GE Healthcare, 17075601) and HIS-tagged proteins with NI-NTA agarose beads
341 (QIAGEN, 30210). Purified proteins were loaded on 4–15% Mini-PROTEAN® TGX™ Precast Protein Gels
342 (Biorad, 4561083DC), stained overnight with Instant Blue (Sigma-Aldrich, ISB1L-1L) and quantified
343 using a BSA standard curve in Image Lab (Biorad). The ubiquitination of DA1, DAR1 and DAR2 and the
344 cleaving assays were performed as described before (Dong et al., 2017). After the ubiquitination step,

8

345 a 1:1 ratio of deubiquitinating enzymes to the ubiquitinated proteins were added and the reaction mix
346 was incubated for 4 h at 30°C. Reactions were stopped by adding 5x SDS sample buffer and boiled for
347 ten min at 90°C. The samples were loaded on 4–15% or 7.5% Mini-PROTEAN® TGX™ Precast Protein
348 Gels (Biorad, 4561083DC). The proteins in the gels were transferred to a PVDF membrane using Trans-
349 blot turbo transfer packs (Biorad, 170-4156) and the membranes were incubated overnight in a 3%
350 skimmed milk (Difco) 1x TBST solution. After blocking, GST-tagged proteins were detected with Anti-
351 GST HRP Conjugate (Sigma-Aldrich, GERPN1236) and MBP-tagged proteins with Anti-MBP Monoclonal
352 Antibody (Biolabs, E8030S) and subsequently with a secondary Rabbit IgG HRP Linked antibody (Sigma-
353 Aldrich, NA934v). The antibodies were used following the manufacturer's instructions.

354 **RNA extraction, cDNA preparation and q-RT-PCR**
355 Total RNA was extracted from flash-frozen seedlings or isolated leaves with TRIzol reagent (Invitrogen).
356 Young seedlings (until 14 DAS) from which the leaves were isolated using a binocular were submerged
357 overnight in RNA Later (Ambion) to prevent RNA degradation. To eliminate the residual genomic DNA
358 present in the preparation, the RNA was treated by RQ1 RNAse-free DNase according to the
359 manufacturer's instructions (Promega) and purified with the RNeasy Mini kit (Qiagen). Complementary
360 DNA was made with the QScript cDNA supermix kit (Quantabio, 95048-100) according to the
361 manufacturer's instructions. Q-RT-PCR was done on a LightCycler 480 (Roche) in 384-well plates with
362 LightCycler 480 SYBR Green I Master (Roche) according to the manufacturer's instructions. Primers
363 were designed with the Primer3 (http://frodo.wi.mit.edu/) (Supplementary Table 1). Data analysis was
364 performed using the ΔΔCT method (Pfaffl, 2001), taking the primer efficiency into account. The
365 expression data was normalized using three reference genes (AT1G13320, AT2G32170, and
366 AT2G28390) according to the GeNorm algorithm (Vandesompele et al., 2002). The statistical analysis
367 (ANOVA, Dunnett's test) was performed in GraphPad Prism 8.1 (www.graphpad.com).

368 **Flow cytometry**
369 The first leaf pair was harvested from 9 to 27 DAS with a three-day interval and frozen in liquid
370 nitrogen. At least three leaves per time point of each biological repeat (n=3) were chopped with a razor
371 blade in 200 µL of Cystain UV Precise P Nuclei Extraction buffer (Sysmex), followed by the addition of
372 800 µL of Cystain UV Precise P staining buffer (Sysmex) and filtering through a 50-mm filter. Nuclei
373 were analyzed with the Cyflow MB flow cytometer (Partec) and the FloMax software. The statistical
374 analysis (ANOVA, Dunnett's test) was performed in GraphPad Prism 8.1 (www.graphpad.com).

375 **GFP pull-down**
376 The IP-MS/MS was based on the protocol from Wendrich et al. (2017). For each pull-down, we used 3
377 g of homogenized Arabidopsis seedlings. The powder was dissolved in 4.5 ml BHB+ buffer
378 supplemented with 4.5 µl benzonase and incubated for 30 min at 4°C. Then, the samples were further
379 mixed three times for 30 s at 18,000 rpm using Ultra-TURRAX miniprobes (IKA). Subsequently, the
380 mixtures were incubated for 30 min at 4°C on an end-over-end rotor. After incubation, the cellular
381 debris was pelleted by two centrifugation steps at 14,000 rpm at 4°C in an Eppendorf centrifuge and
382 further withheld by a 0.45-µm filter (Sartorius). The protein content was measured (OD 595) using a
383 Bradford (Biorad) standard curve and equal amounts of proteins were incubated with 50 µl pre-
384 washed anti-GFP-beads (µMacs, Miltenyi Biotec) for 1 h at 4°C in an end-over-end shaker. To isolate
385 the beads, the columns were placed in the magnetic holder and washed four times with 200 µl BHB+
386 buffer and two times with 500 µl NH_4HCO_3 buffer. The purified proteins were eluted stepwise by 50 µl

387   95°C hot NH_4HCO_3 each time until no more beads pass through the column. Then, 4 µl Tryp/LysC mix
388   (Promega) was added and the proteins were digested on-bead for 4 h at 37°C with agitation (800 rpm)
389   on an Eppendorf thermomixer. The digested mix was loaded again on the µMacs column attached to
390   the magnetic holder to separate the eluate from beads. The eluate was collected in a new protein low
391   binding Eppendorf tube and additionally 2 µl Tryp/LysC was added for an overnight digestion at 37°C
392   with agitation (800 rpm) in an Eppendorf thermomixer. Finally, the samples were snap-frozen in liquid
393   nitrogen and freeze-dried in a Speedvac (Labconco). Protein identification and data analysis were
394   performed as described before (Van Leene et al., 2015).

Acknowledgements

Figure legends

401   **Figure 1. UBP12 and UBP13 interact with DA1, DAR1 and DAR2.** (A-C) Enrichment of the bait, UBP12
402   and UBP13 compared to the control after immunoprecipitation in (A) *35S::GFP-DA1* (FDR=0.01, S0=1,
403   permutation-based FDR-corrected t-test, Figure 1-source data 1), (B) *35S::GFP-DAR1* (FDR=0.01, S0=1,
404   permutation-based FDR-corrected t-test, Figure 1-source data 1) or (C) *35S::GFP-DAR2* (FDR=0.05,
405   S0=1, permutation-based FDR-corrected t-test, Figure 1-source data 1) seedlings.

406   **Figure 2. Regulation of leaf size by UBP12 and UBP13.** (A) Twenty-one-day-old plants of Col-0, *da1-1*
407   and homozygous (+/+) or heterozygous (+/-) *UBP12* and *UBP13* overexpression lines. Scale bar
408   represents 1 cm, homozygous and heterozygous plants of the same single locus line are linked in the
409   figure. (B) Leaf area measurements of Col-0 and *ubp12-2*, n=3 biological repeats with >10 plants per
410   repeat. (C) Percentage differences of leaf area, cell area and cell number of *ubp12-2*, *35S::UBP12_3.1*,
411   *35S::UBP12_3.2*, *35S::UBP13_1.1* and *35S::UBP13_3.2* compared to Col-0, n=3 biological repeats with
412   3 representative leaves per repeat. (D) Relative frequencies of LN transformed cell area distribution of
413   Col-0, *35S::UBP12_3.1*, *35S::UBP12_3.2*, *35S::UBP13_1.1* and *35S::UBP13_3.2* in 1 μm^2 bin sizes, n=3
414   biological repeats with 3 representative leaves per repeat. Bars represent the SEM; * indicates p-value
415   < 0.05, ANOVA (Figure 2-source data 1).

416   **Figure 3. UBP12 and UBP13 regulate the onset of endoreduplication.** (A) Ploidy distribution of nuclear
417   DNA in Col-0, *35S::UBP12_3.1* and *35S::UBP13_1.1*. (B-C) Fractional difference in expression of cell
418   proliferation markers in *35S::UBP12_3.1* and *35S::UBP13_1.1* compared to Col-0 at (B) 9 and (C) 12
419   DAS. Bars represent the SEM, n=3 biological repeats with > 3 leaves per repeat; a, b and c indicate a
420   significant difference in 2C, 4C and 8C, respectively; * indicates p-value < 0.05, ANOVA, (Figure 3-source
421   data 1).

422   **Figure 4. Deubiquitination of DA1, DAR1 and DAR2 by UBP12 and UBP13.** (A-C) *In vitro*
423   deubiquitination assays with GST-UBP12, GST-UBP12[C208S], GST-UBP13 or GST-UBP13[C207S] of (A) HIS-
424   MBP-DA1, (B) HIS-MBP-DAR1 and (C) HIS-MBP-DAR2. (D) Deubiquitination assay with GST-UBP12, GST-
425   UBP13, GST-UBP3, GST-UBP15 and GST-UBP24 of HIS-MBP-DA1.

Figure 5. Cleaving assay on UBP12 and UBP13. (A) *In vitro* cleaving assay on GST-UBP12, GST-UBP12^{C208S}, GST-UBP13 and GST-UBP13^{C207S} by HIS-MBP-DA1 and the peptidase-deficient HIS-MBP-DA1^{H418A,H422A}. (B) Twenty-one-day-old plants of Col-0, *35S::GFP-DA1*, *35S::UBP12_3.1/35S::GFP-DA1*, *35S::UBP12_3.2/35S::GFP-DA1*, *35S::UBP13_2.1/35S::GFP-DA1* and *35S::UBP13_2.2/35S::GFP-DA1* homozygous (+/+) and heterozygous (+/-) double overexpression lines. Scale bar represents 1cm.

Figure 6. Model of UBP12 and UBP13 levels on leaf area and cellular phenotypes. Molecular balance and leaf phenotypes in (A) wild-type conditions, (B) high *UBP12* and *UBP13* expression lines and (C) lower levels of *UBP12* and *UBP13*.

Figure supplement legends

Figure 1-figure supplement 1. Overlap between potential interactors of DA1, DAR1 and DAR2.

Figure 1-figure supplement 2. MS/MS counts of DA1, DAR1 and DAR2 baits from GFP-DA1, GFP-DAR1 and GFP-DAR2 pull-downs, respectively (Bars represent the SEM; n=3 biological repeats; Figure 1-source data 2).

Figure 1-figure supplement 3. Percentage coverage of the DA1, DAR1 and DAR2 baits from GFP-DA1, GFP-DAR1 and GFP-DAR2 pull-downs, respectively (Bars represent the SEM; n=3 biological repeats; Figure 1-source data 2).

Figure 1-figure supplement 4. Relative expression levels of *UBP12*, *UBP13*, *DA1*, *DAR1* and *DAR2* throughout leaf development, scaled to the lowest value (DAR2, 5 DAS; Figure 1-source data 2). Scale bar represents 1 cm. Bars represent the SEM; n=3 biological repeats)

Figure 2-figure supplement 1. *UBP12* and *UBP13* transcript levels in Col-0, *da1-1*, *35S::UBP12_3.1*, *35S::UBP12_3.2*, *35S::UBP13_1.1* and *35S::UBP13_3.2* overexpression lines. Bars represent the SEM; * indicates p-value < 0.05, ANOVA; (Figure 2-source data 2).

Figure 2-figure supplement 2. Leaf area measurements of *ubp12-1*, compared to Col-0, n=3 biological repeats with >10 plants per repeat. Bars represent the SEM; * indicates p-value < 0.05, ANOVA; (Figure 2-source data 2).

Figure 2-figure supplement 3. Leaf area measurements of *ubp13-1*, compared to Col-0, n=3 biological repeats with >10 plants per repeat. Bars represent the SEM; * indicates p-value < 0.05, ANOVA; (Figure 2-source data 2).

Figure 2-figure supplement 4. Leaf area measurements of *ubp13-2* and compared to Col-0, n=3 biological repeats with >10 plants per repeat. Bars represent the SEM; * indicates p-value < 0.05, ANOVA; (Figure 2-source data 2).

Figure 2-figure supplement 5. Leaf area measurements of *ubp13-3* compared to Col-0, n=3 biological repeats with >10 plants per repeat. Bars represent the SEM; * indicates p-value < 0.05, ANOVA; (Figure 2-source data 2).

Figure 2-figure supplement 6. Representations of abaxial leaf epidermal cells of Col-0, homozygous *35S::UBP12_3.1*, homozygous *35S::UBP12_3.2*, heterozygous *35S::UBP13_1.1* and heterozygous *35S::UBP13_3.2*. (+/-) and (+/+) indicate heterozygous and homozygous plants, respectively.

463   **Figure 2-figure supplement 7.** Representations of abaxial leaf epidermal cells of Col-0 and the
464   homozygous *35S::UBP13_1.1*, (+/+) indicates homozygous plants

465   **Figure 2-figure supplement 8.** Cell size distribution plot of Col-0 and *ubp12-2*, n=3 biological repeats
466   with 3 representative leaves per repeat. Bars represent the SEM; * indicates p-value < 0.05, ANOVA;
467   (Figure 2-source data 2).

468   **Figure 3-figure supplement 1.** Endoreduplication index of *35S::UBP12_3.1* leaf nuclei compared to Col-
469   0. Bars represent the SEM; n=3 biological repeats with > 3 leaves per repeat; * indicates p-value < 0.05,
470   ANOVA, (Figure 3-source data 2).

471   **Figure 3-figure supplement 2.** Endoreduplication index of *35S::UBP13_1.1* leaf nuclei compared to Col-
472   0. Bars represent the SEM; n=3 biological repeats with > 3 leaves per repeat; * indicates p-value < 0.05,
473   ANOVA, (Figure 3-source data 2).

474   **Figure 3-figure supplement 3.** Relative expression levels of cell proliferation markers in Col-0,
475   *35S::UBP12_3.1* and *35S::UBP13_1.1* at 15 DAS. Bars represent the SEM; n=3 biological repeats with >
476   3 leaves per repeat; * indicates p-value < 0.05, ANOVA, (Figure 3-source data 2).

477   **Figure 3-figure supplement 4.** Relative expression levels of cell proliferation markers in Col-0,
478   *35S::UBP12_3.1* and *35S::UBP13_1.1* at 18 DAS. Bars represent the SEM; n=3 biological repeats with >
479   3 leaves per repeat; * indicates p-value < 0.05, ANOVA, (Figure 3-source data 2).

480   **Figure 5-figure supplement 1.** Relative expression levels of *DA1*, *UBP12* and *UBP13* in the double
481   *35S::GFP-DA1_35S::UBP12* and *35S::GFP-DA1_35S::UBP13* overexpression lines. n=3 biological repeats
482   with > 3 leaves per repeat, * indicates p-value < 0.05 compared to the expression levels in Col-0,
483   ANOVA, (Figure 5-source data 1).

Source data files

485   **Figure 1-source data 1:** List of DA1, DAR1, DAR2 interactors and LFQ intensities by MS/MS

486   **Figure 1-source data 2:** MS/MS counts of DA1, DAR1 and DAR2; protein coverage of DA1, DAR1 and
487   DAR2; relative expression levels of *DA1*, *DAR1*, *DAR2*, *UBP12* and *UBP13* during leaf development

488   **Figure 2-source data 1:** Leaf area analysis and statistics of Col-0 and *ubp12-2*; leaf area analysis and
489   statistics of Col-0, *35S::UBP12_3.1*, *35S::UBP12_3.2*, *35S::UBP13_1.1* and *35S::UBP13_3.2*; cellular
490   analysis and statistics of Col-0, *35S::UBP12_3.1*, *35S::UBP12_3.2*, *35S::UBP13_1.1* and *35S::UBP13_3.2*;
491   cellular analysis of *ubp12-2*, relative frequency of the pavement cell area and statistics of Col-0,
492   *35S::UBP12_3.1*, *35S::UBP12_3.2*, *35S::UBP13_1.1* and *35S::UBP13_3.2*.

493   **Figure 2-source data 2:** Q-RT-PCR data and statistics of *UBP12* and *UBP13* expression in Col-0, *da1-1*,
494   *35S::UBP12_3.1*, *35S::UBP12_3.2*, *35S::UBP13_1.1* and *35S::UBP13_3.2* overexpression lines; leaf area
495   data and statistics of *ubp12-1*; leaf area data and statistics of *ubp13-1*; leaf area data and statistics of
496   *ubp13-2*; leaf area data and statistics of *ubp13-3*; relative frequency of *ubp12-2* pavement cell area
497   data and statistics.

498   **Figure 3-source data 1:** Flow cytometry counts and statistics; Q-RT-PCR data and statistics of
499   proliferation markers in developing leaves (9 DAS and 12 DAS).

500 **Figure 3-source data 2:** Endoreduplication index calculations and statistics; Q-RT-PCR data and
501 statistics of proliferation markers in developing leaves (15 DAS and 18 DAS).

502 **Figure 5-source data 1: :** Q-RT-PCR data and statistics of *DA1*, *UBP12* and *UBP13* expression in Col-0,
503 *35S::GFP-DA1*, *35S::UBP12_3.1/35S::GFP-DA1*, *35S::UBP12_3.2/35S::GFP-DA1*,
504 *35S::UBP13_2.1/35S::GFP-DA1* and *35S::UBP13_2.2/35S::GFP-DA1.*

Supplementary tables
506 Supplementary Table 1: Primer list

507 Supplementary Table 1: Conditions recombinant protein production

References

509 An Z, Liu Y, Ou Y, Li J, Zhang B, Sun D, Sun Y, Tang W. 2018. Regulation of the stability of RGF1 receptor
510 by the ubiquitin-specific proteases UBP12/UBP13 is critical for root meristem maintenance.
511 *Proceedings of the National Academy of Sciences of the United States of America* **115:** 1123-1128.
512 DOI: https://doi.org/10.1073/pnas.1714177115
513 Anastasiou E, Kenz S, Gerstung M, MacLean D, Timmer J, Fleck C, Lenhard M. 2007. Control of plant
514 organ size by *KLUH/CYP78A5*-dependent intercellular signaling. *Developmental Cell* **13:** 843-856.
515 DOI: https://doi.org/10.1016/j.devcel.2007.10.001
516 Andriankaja M, Dhondt S, De Bodt S, Vanhaeren H, Coppens F, De Milde L, Mühlenbock P, Skirycz A,
517 Gonzalez N, Beemster GTS, Inzé D. 2012. Exit from proliferation during leaf development in
518 *Arabidopsis thaliana*: a not-so-gradual process. *Developmental Cell* **22:** 64-78. DOI:
519 https://doi.org/10.1016/j.devcel.2011.11.011
520 Callis J. 2014. The ubiquitination machinery of the ubiquitin system. *The Arabidopsis book* **12:** e0174.
521 DOI: https://doi.org/10.1199/tab.0174
522 Callis J, Carpenter T, Sun C-W, Vierstra RD. 1995. Structure and evolution of genes encoding
523 polyubiquitin and ubiquitin-like proteins in *Arabidopsis thaliana* ecotype Columbia. *Genetics* **139:**
524 921-939. DOI
525 Callis J, Raasch JA, Vierstra RD. 1990. Ubiquitin extension proteins of *Arabidopsis thaliana*. Structure,
526 localization, and expression of their promoters in transgenic tobacco. *Journal of Biological Chemistry*
527 **265:** 12486-12493. DOI
528 Clague MJ, Urbé S, Komander D. 2019. Breaking the chains: deubiquitylating enzyme specificity begets
529 function. *Nature Reviews Molecular Cell Biology* **20:** 338-352. DOI: https://doi.org/10.1038/s41580-
530 019-0099-1
531 Crespo-Yàñez X, Aguilar-Gurrieri C, Jacomin A-C, Journet A, Mortier M, Taillebourg E, Soleilhac E,
532 Weissenhorn W, Fauvarque M-O. 2018. CHMP1B is a target of USP8/UBPY regulated by ubiquitin
533 during endocytosis. *PLoS Genetics* **14:** e1007456. DOI:
534 https://doi.org/10.1371/journal.pgen.1007456
535 Cui X, Lu F, Li Y, Xue Y, Kang Y, Zhang S, Qiu Q, Cui X, Zheng S, Liu B, Xu X, Cao X. 2013. Ubiquitin-specific
536 proteases UBP12 and UBP13 act in circadian clock and photoperiodic flowering regulation in
537 Arabidopsis. *Plant Physiology* **162:** 897-906. DOI: https://doi.org/10.1104/pp.112.213009
538 Derkacheva M, Liu S, Figueiredo DD, Gentry M, Mozgova I, Nanni P, Tang M, Mannervik M, Köhler C,
539 Hennig L. 2016. H2A deubiquitinases UBP12/13 are part of the *Arabidopsis* polycomb group protein
540 system. *Nature Plants* **2:** 16126. DOI: https://doi.org/10.1038/nplants.2016.126
541 Doerner P, Jørgensen J-E, You R, Steppuhn J, Lamb C. 1996. Control of root growth and development
542 by cyclin expression. *Nature* **380:** 520-523. DOI: https://doi.org/10.1038/380520a0
543 Dong H, Dumenil J, Lu F-H, Na L, Vanhaeren H, Naumann C, Klecker M, Prior R, Smith C, McKenzie N,
544 Saalbach G, Chen L, Xia T, Gonzalez N, Seguela M, Inzé D, Dissmeyer N, Li Y, Bevan MW. 2017.
545 Ubiquitylation activates a peptidase that promotes cleavage and destabilization of its activating E3

ligases and diverse growth regulatory proteins to limit cell proliferation in *Arabidopsis*. *Genes & Development* **31:** 197-208. DOI: https://doi.org/10.1101/gad.292235.116

Donnelly PM, Bonetta D, Tsukaya H, Dengler RE, Dengler NG. 1999. Cell cycling and cell enlargement in developing leaves of *Arabidopsis*. *Developmental Biology* **215:** 407-419. DOI: https://doi.org/10.1006/dbio.1999.9443

Du L, Li N, Chen L, Xu Y, Li Y, Zhang Y, Li C, Li Y. 2014. The ubiquitin receptor DA1 regulates seed and organ size by modulating the stability of the ubiquitin-specific protease UBP15/SOD2 in *Arabidopsis*. *Plant Cell* **26:** 665-677. DOI: https://doi.org/10.1105/tpc.114.122663

Ewan R, Pangestuti R, Thornber S, Craig A, Carr C, O'Donnell L, Zhang C, Sadanandom A. 2011. Deubiquitinating enzymes AtUBP12 and AtUBP13 and their tobacco homologue NtUBP12 are negative regulators of plant immunity. *New Phytologist* **191:** 92-106. DOI: https://doi.org/10.1111/j.1469-8137.2011.03672.x

Horiguchi G, Kim G-T, Tsukaya H. 2005. The transcription factor AtGRF5 and the transcription coactivator AN3 regulate cell proliferation in leaf primordia of *Arabidopsis thaliana*. *Plant Journal* **43:** 68-78. DOI: https://doi.org/10.1111/j.1365-313X.2005.02429.x

Huang OW, Cochran AG. 2013. Regulation of deubiquitinase proteolytic activity. *Current Opinion in Structural Biology* **23:** 806-811. DOI: https://doi.org/10.1016/j.sbi.2013.07.012

Isono E, Nagel M-K. 2014. Deubiquitylating enzymes and their emerging role in plant biology. *Frontiers in Plant Science* **5:** 56. DOI: https://doi.org/10.3389/fpls.2014.00056

Jeong JS, Jung C, Seo JS, Kim J-K, Chua N-H. 2017. The deubiquitinating enzymes UBP12 and UBP13 positively regulate MYC2 levels in jasmonate responses. *Plant Cell* **29:** 1406-1424. DOI: https://doi.org/10.1105/tpc.17.00216

Joo H-Y, Zhai L, Yang C, Nie S, Erdjument-Bromage H, Tempst P, Chang C, Wang H. 2007. Regulation of cell cycle progression and gene expression by H2A deubiquitination. *Nature* **449:** 1068-1072. DOI: https://doi.org/10.1038/nature06256

Kazama T, Ichihashi Y, Murata S, Tsukaya H. 2010. The mechanism of cell cycle arrest front progression explained by a *KLUH/CYP78A5*-dependent mobile growth factor in developing leaves of *Arabidopsis thaliana*. *Plant & Cell Physiology* **51:** 1046-1054. DOI: https://doi.org/10.1093/pcp/pcq051

Komander D, Clague MJ, Urbé S. 2009. Breaking the chains: structure and function of the deubiquitinases. *Nature Reviews Molecular Cell Biology* **10:** 550-563. DOI: https://doi.org/10.1038/nrm2731

Lee C-M, Li M-W, Feke A, Liu W, Saffer AM, Gendron JM. 2019. GIGANTEA recruits the UBP12 and UBP13 deubiquitylases to regulate accumulation of the ZTL photoreceptor complex. *Nature Communications* **10:** 3750. DOI: https://doi.org/10.1038/s41467-019-11769-7

Li Y, Zheng L, Corke F, Smith C, Bevan MW. 2008. Control of final seed and organ size by the *DA1* gene family in *Arabidopsis thaliana*. *Genes & Development* **22:** 1331-1336. DOI: https://doi.org/10.1101/gad.463608

Liu Y, Wang F, Zhang H, He H, Ma L, Deng X. 2008. Functional characterization of the Arabidopsis *ubiquitin-specific protease* gene family reveals specific role and redundancy of individual members in development. *Plant Journal* **55:** 844-856. DOI: https://doi.org/10.1111/j.1365-313X.2008.03557.x

Marzec M. 2016. Perception and Signaling of Strigolactones. *Frontiers in Plant Science* **7:** 1260. DOI: https://doi.org/10.3389/fpls.2016.01260

Mizukami Y, Fischer RL. 2000. Plant organ size control: *AINTEGUMENTA* regulates growth and cell numbers during organogenesis. *Proceedings of the National Academy of Sciences of the United States of America* **97:** 942-947. DOI: https://doi.org/10.1073/pnas.97.2.942

Nagels Durand A, Pauwels L, Goossens A. 2016. The ubiquitin system and jasmonate signaling. *Plants* **5:** 6. DOI: https://doi.org/10.3390/plants5010006
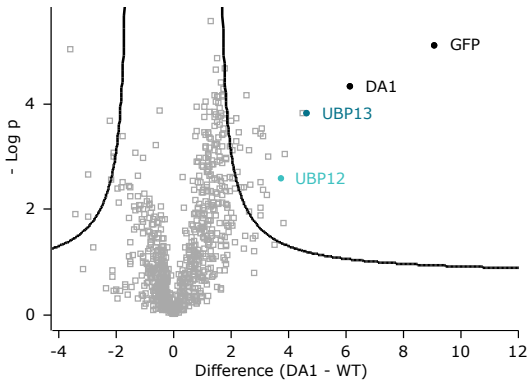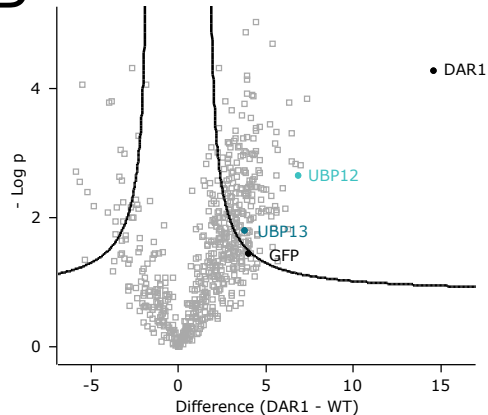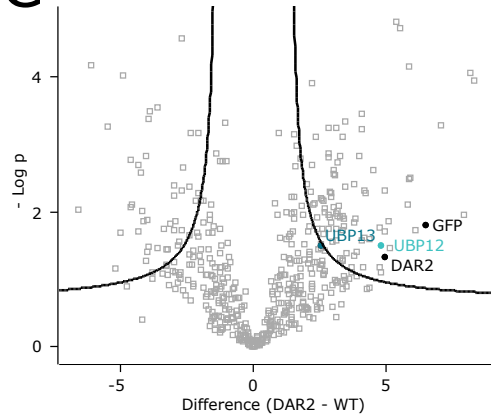
Nijman SMB, Huang TT, Dirac AMG, Brummelkamp TR, Kerkhoven RM, D'Andrea AD, Bernards R. 2005. The deubiquitinating enzyme USP1 regulates the Fanconi anemia pathway. *Molecular Cell* **17:** 331-339. DOI: https://doi.org/10.1016/j.molcel.2005.01.008
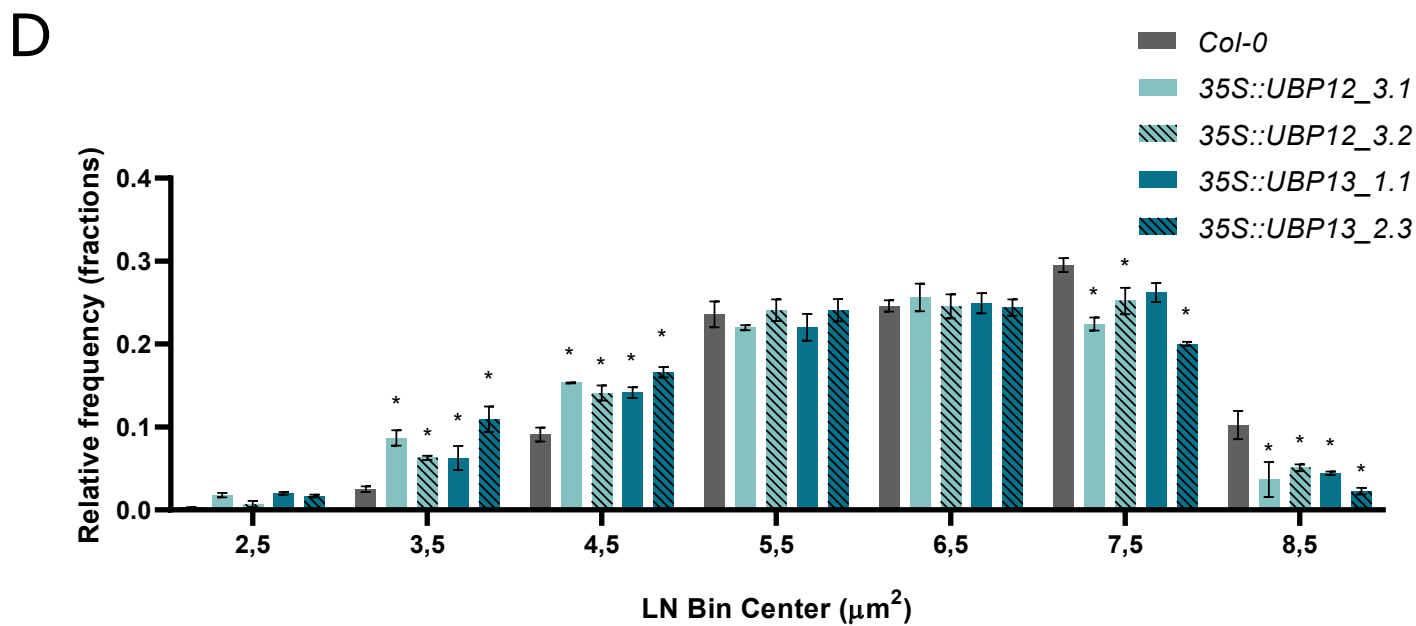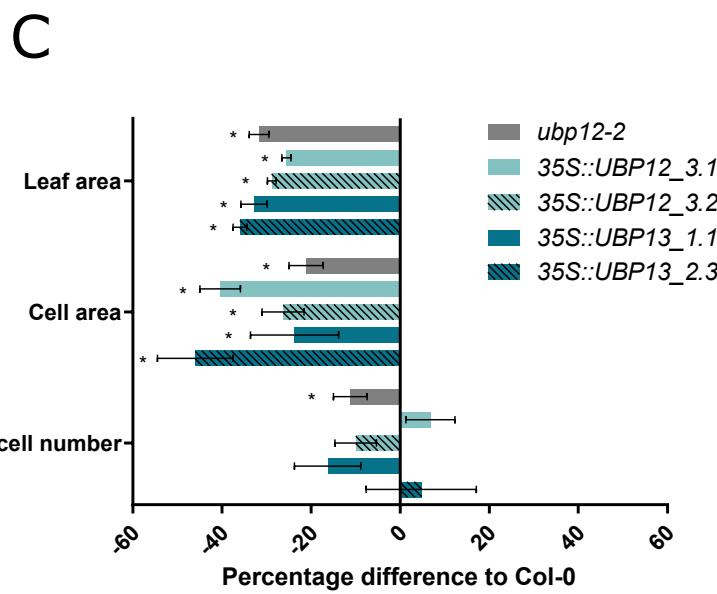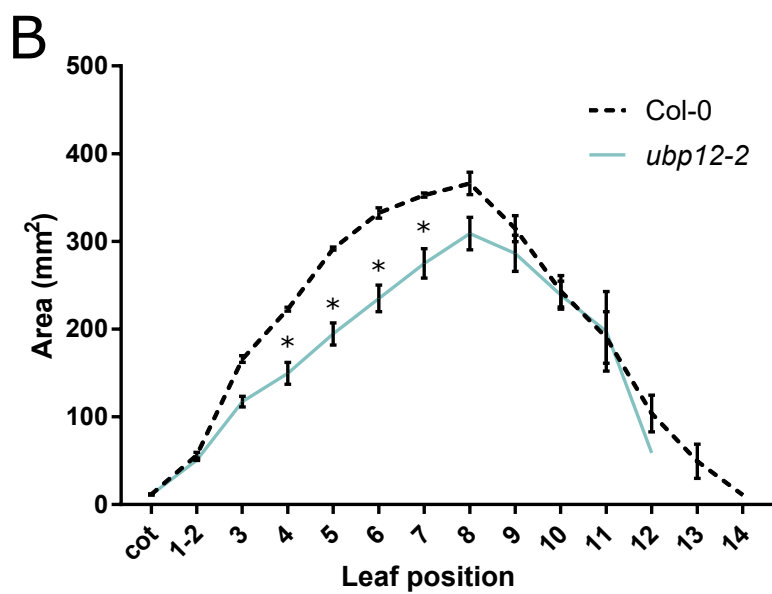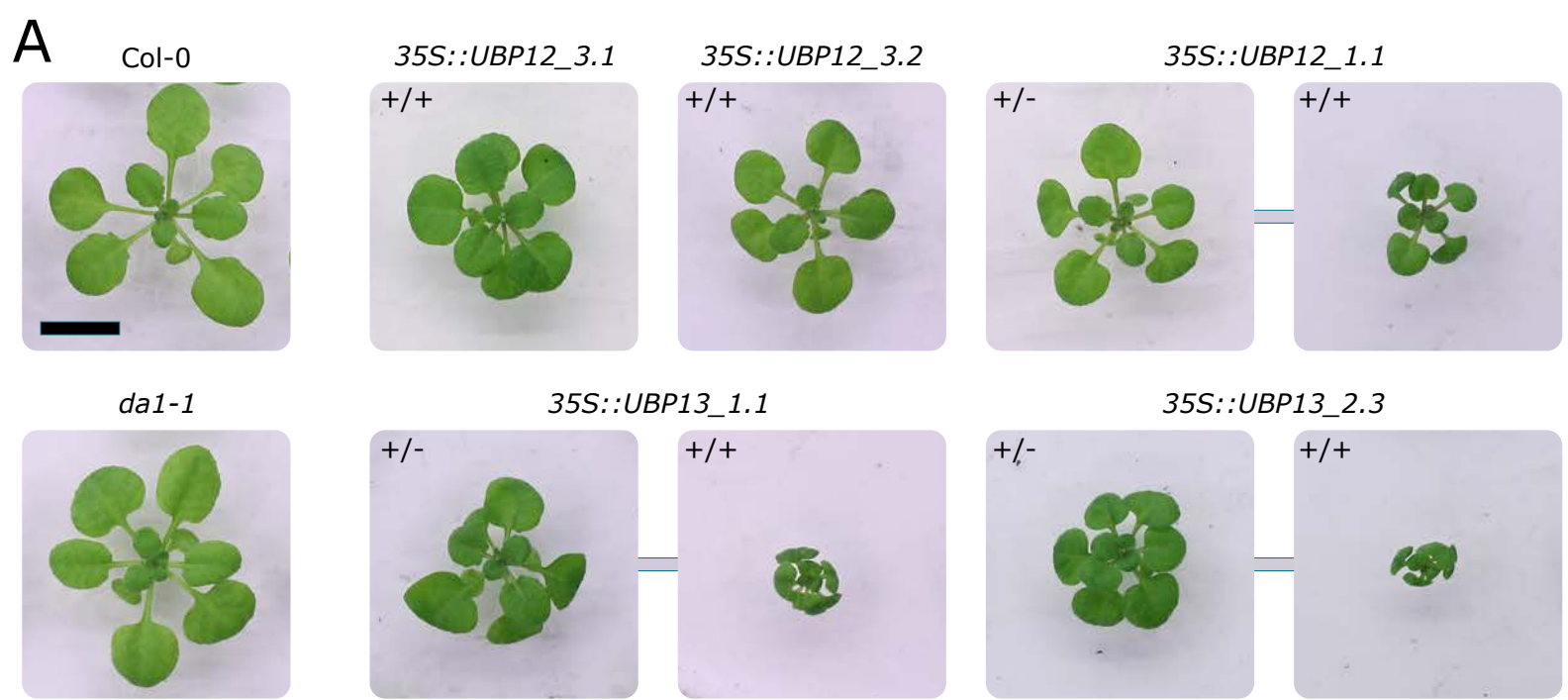
596 Park S-H, Jeong JS, Seo JS, Park BS, Chua N-H. 2019. Arabidopsis ubiquitin-specific proteases UBP12
597   and UBP13 shape ORE1 levels during leaf senescence induced by nitrogen deficiency. *New
598   Phytologist* **223:** 1447-1460. DOI: https://doi.org/10.1111/nph.15879
599 Peng Y, Chen L, Lu Y, Wu Y, Dumenil J, Zhu Z, Bevan MW, Li Y. 2015. The ubiquitin receptors DA1, DAR1,
600   and DAR2 redundantly regulate endoreduplication by modulating the stability of TCP14/15 in
601   Arabidopsis. *Plant Cell* **27:** 649-662. DOI: https://doi.org/10.1105/tpc.114.132274
602 Pfaffl MW. 2001. A new mathematical model for relative quantification in real-time RT-PCR. *Nucleic
603   Acids Research* **29:** e45. DOI: https://doi.org/10.1093/nar/29.9.e45
604 Row PE, Prior IA, McCullough J, Clague MJ, Urbé S. 2006. The ubiquitin isopeptidase UBPY regulates
605   endosomal ubiquitin dynamics and is essential for receptor down-regulation. *Journal of Biological
606   Chemistry* **281:** 12618-12624. DOI: https://doi.org/10.1074/jbc.M512615200
607 Salehin M, Bagchi R, Estelle M. 2015. SCF$^{TIR1/AFB}$-based auxin perception: mechanism and role in plant
608   growth and development. *Plant Cell* **27:** 9-19. DOI: https://doi.org/10.1105/tpc.114.133744
609 Santner A, Estelle M. 2010. The ubiquitin-proteasome system regulates plant hormone signaling. *Plant
610   Journal* **61:** 1029-1040. DOI: https://doi.org/10.1111/j.1365-313X.2010.04112.x
611 Shaul O, Mironov V, Burssens S, Van Montagu M, Inzé D. 1996. Two *Arabidopsis* cyclin promoters
612   mediate distinctive transcriptional oscillation in synchronized tobacco BY-2 cells. *Proceedings of the
613   National Academy of Sciences of the United States of America* **93:** 4868-4872. DOI:
614   https://doi.org/10.1073/pnas.93.10.4868
615 Shimada TL, Shimada T, Hara-Nishimura I. 2010. A rapid and non-destructive screenable marker, FAST,
616   for identifying transformed seeds of *Arabidopsis thaliana*. *Plant Journal* **61:** 519-528. DOI:
617   https://doi.org/10.1111/j.1365-313X.2009.04060.x
618 Shu K, Yang W. 2017. E3 ubiquitin ligases: ubiquitous actors in plant development and abiotic stress
619   responses. *Plant & Cell Physiology* **58:** 1461-1476. DOI: https://doi.org/10.1093/pcp/pcx071
620 Swatek KN, Komander D. 2016. Ubiquitin modifications. *Cell Research* **26:** 399-422. DOI:
621   https://doi.org/10.1038/cr.2016.39
622 Van Leene J, Eeckhout D, Cannoot B, De Winne N, Persiau G, Van De Slijke E, Vercruysse L, Dedecker
623   M, Verkest A, Vandepoele K, Martens L, Witters E, Gevaert K, De Jaeger G. 2015. An improved
624   toolbox to unravel the plant cellular machinery by tandem affinity purification of *Arabidopsis* protein
625   complexes. *Nature Protocols* **10:** 169-187. DOI: https://doi.org/10.1038/nprot.2014.199
626 Vandesompele J, De Preter K, Pattyn F, Poppe B, Van Roy N, De Paepe A, Speleman F. 2002. Accurate
627   normalization of real-time quantitative RT-PCR data by geometric averaging of multiple internal
628   control genes. *Genome Biology* **3:** research0034-research0034.11. DOI: https://doi.org/10.1186/gb-
629   2002-3-7-research0034
630 Vanhaeren H, Nam YJ, De Milde L, Chae E, Storme V, Weigel D, Gonzalez N, Inzé D. 2017. Forever young:
631   the role of ubiquitin receptor DA1 and E3 ligase Big Brother in controlling leaf growth and
632   development. *Plant Physiology* **173:** 1269-1282. DOI: https://doi.org/10.1104/pp.16.01410
633 Vercruyssen L, Tognetti VB, Gonzalez N, Van Dingenen J, De Milde L, Bielach A, De Rycke R, Van
634   Breusegem F, Inzé D. 2015. GROWTH REGULATING FACTOR5 stimulates Arabidopsis chloroplast
635   division, photosynthesis, and leaf longevity. *Plant Physiology* **167:** 817-832. DOI:
636   https://doi.org/10.1104/pp.114.256180
637 Vierstra RD. 2009. The ubiquitin-26S proteasome system at the nexus of plant biology. *Nature Reviews
638   Molecular Cell Biology* **10:** 385-397. DOI: https://doi.org/10.1038/nrm2688
639 Wang F, Deng XW. 2011. Plant ubiquitin-proteasome pathway and its role in gibberellin signaling. *Cell
640   Research* **21:** 1286-1294. DOI: https://doi.org/10.1038/cr.2011.118
641 Wendrich JR, Boeren S, Möller BK, Weijers D, De Rybel B. 2017. In vivo identification of plant protein
642   complexes using IP-MS/MS. *Methods in Molecular Biology* **1497:** 147-158. DOI:
643   https://doi.org/10.1007/978-1-4939-6469-7_14
644 Yan N, Doelling JH, Falbel TG, Durski AM, Vierstra RD. 2000. The ubiquitin-specific protease family from
645   Arabidopsis. *At*UBP1 and 2 are required for the resistance to the amino acid analog canavanine. *Plant
646   Physiology* **124:** 1828-1843. DOI: https://doi.org/10.1104/pp.124.4.1828
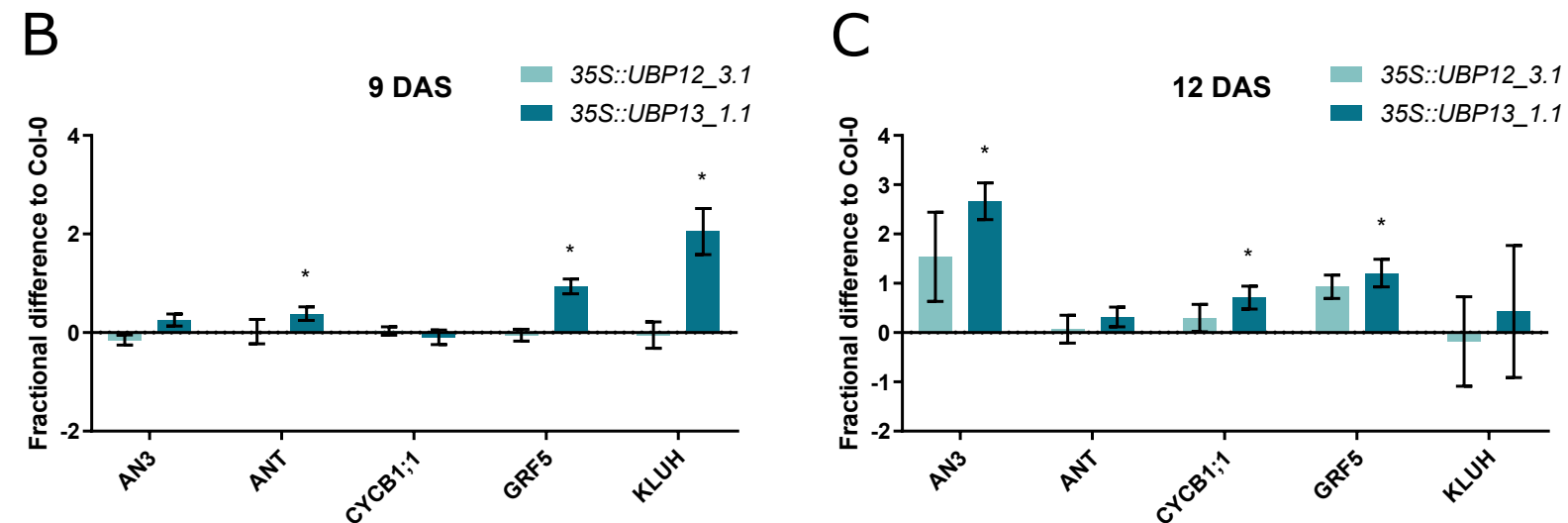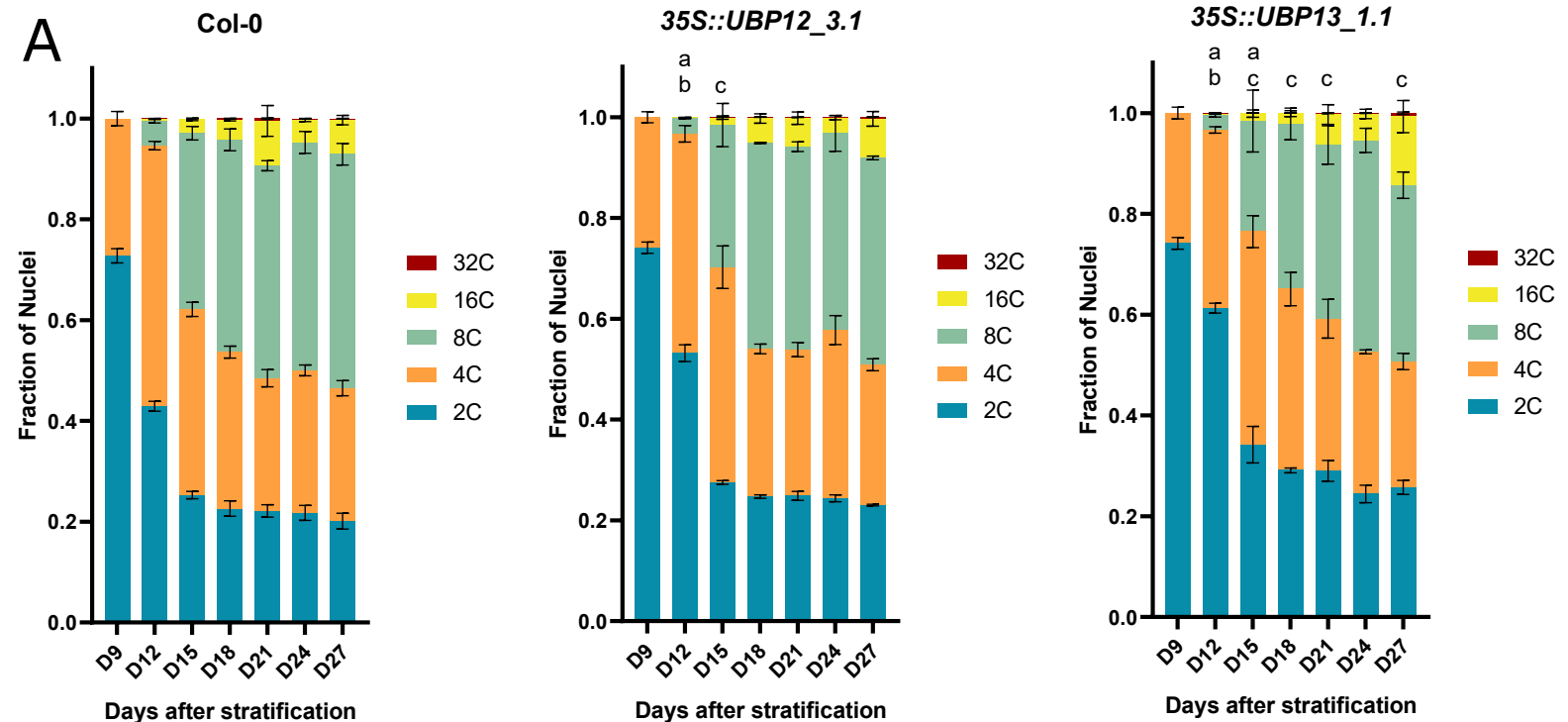
647 Zhou H, Zhao J, Cai J, Patil SB. 2017. UBIQUITIN-SPECIFIC PROTEASES function in plant development
648   and stress responses. *Plant Molecular Biology* **94:** 565-576. DOI: https://doi.org/10.1007/s11103-
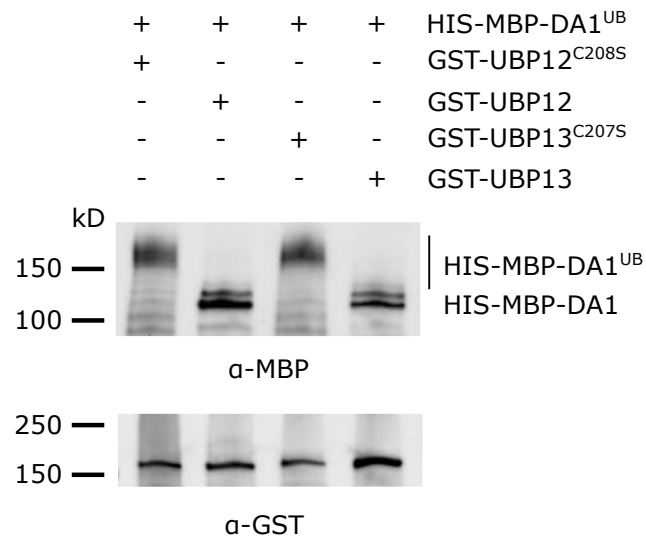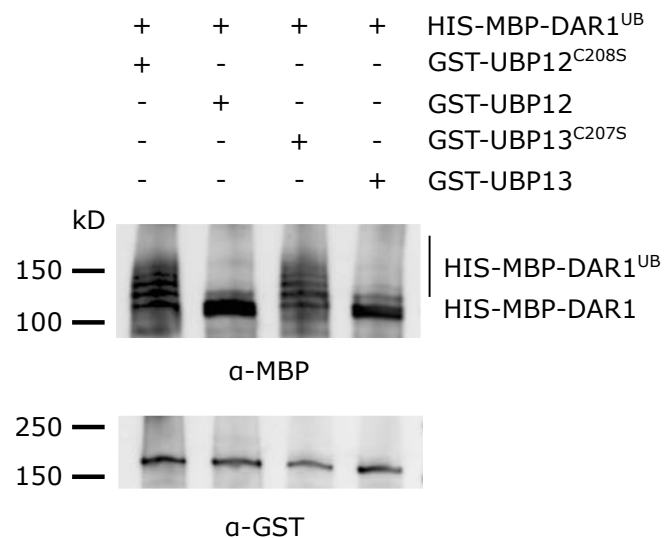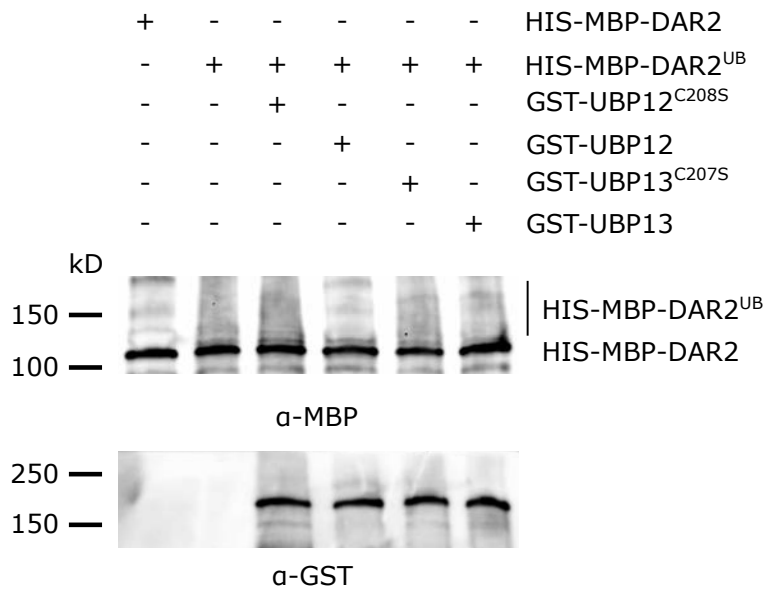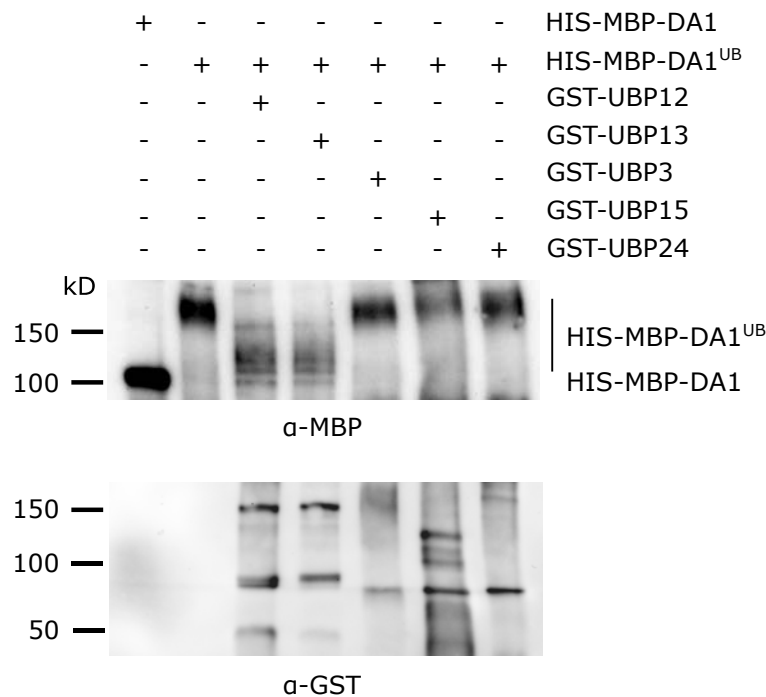649   017-0633-5
650 Zhu P, Zhou W, Wang J, Puc J, Ohgi KA, Erdjument-Bromage H, Tempst P, Glass CK, Rosenfeld MG.
651   2007. A histone H2A deubiquitinase complex coordinating histone acetylation and H1 dissociation in
652   transcriptional   regulation.   *Molecular   Cell*   **27:**   609-621.   DOI:
653   https://doi.org/10.1016/j.molcel.2007.07.024

654

A

+	+	+	+	HIS-MBP-DA1^{UB}
+	-	-	-	GST-UBP12^{C208S}
-	+	-	-	GST-UBP12
-	-	+	-	GST-UBP13^{C207S}
-	-	-	+	GST-UBP13

HIS-MBP-DA1^{UB}
HIS-MBP-DA1

α-MBP

α-GST

B

+	+	+	+	HIS-MBP-DAR1^{UB}
+	-	-	-	GST-UBP12^{C208S}
-	+	-	-	GST-UBP12
-	-	+	-	GST-UBP13^{C207S}
-	-	-	+	GST-UBP13

HIS-MBP-DAR1^{UB}
HIS-MBP-DAR1

α-MBP

α-GST

C

+	-	-	-	-	-	HIS-MBP-DAR2
-	+	+	+	+	+	HIS-MBP-DAR2^{UB}
-	-	+	-	-	-	GST-UBP12^{C208S}
-	-	-	+	-	-	GST-UBP12
-	-	-	-	+	-	GST-UBP13^{C207S}
-	-	-	-	-	+	GST-UBP13

HIS-MBP-DAR2^{UB}
HIS-MBP-DAR2

α-MBP

α-GST

D

+	-	-	-	-	-	-	HIS-MBP-DA1
-	+	+	+	+	+	+	HIS-MBP-DA1^{UB}
-	-	+	-	-	-	-	GST-UBP12
-	-	-	+	-	-	-	GST-UBP13
-	-	-	-	+	-	-	GST-UBP3
-	-	-	-	-	+	-	GST-UBP15
-	-	-	-	-	-	+	GST-UBP24

HIS-MBP-DA1^{UB}
HIS-MBP-DA1

α-MBP

α-GST

A — α-GST / α-MBP

+	-	+	-	+	-	+	-	HIS-MBP-DA1^{UB}
-	+	-	+	-	+	-	+	HIS-MBP-DA1$^{H418A, H422A\ UB}$
+	+	-	-	-	-	-	-	GST-UBP12
-	-	+	+	-	-	-	-	GST-UBP12^{C208S}
-	-	-	-	+	+	-	-	GST-UBP13
-	-	-	-	-	-	+	+	GST-UBP13^{C207S}
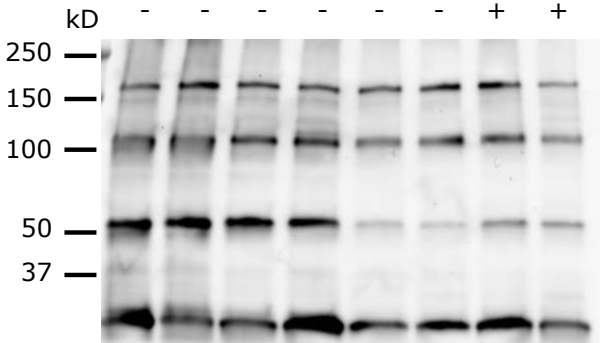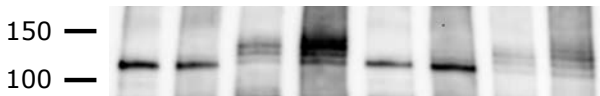
B — Col-0

35S::GFP-DA1   *35S::UBP13_2.1*   *35S::UBP13_2.2*

35S::UBP12_3.1   *35S::UBP12_3.2*

35S::GFP-DA1 background

A

DA1
DAR1
DAR2

Ub

Ub

UBP12
UBP13

UBP12
UBP13

Ub Ub Ub Ub DA1
Ub Ub Ub Ub DAR1
Ub Ub Ub Ub DAR2

UBP15   TCP15   TCP22

B

DA1
DAR1
DAR2

Ub Ub
Ub
Ub

UBP12
UBP13

UBP12
UBP13

Ub
Ub
Ub

Ub Ub Ub Ub DA1
Ub Ub Ub Ub DAR1
Ub Ub Ub Ub DAR2

UBP15   TCP15   TCP22

C

DA1
DAR1
DAR2

UBP12
UBP13

UBP12
UBP13

Ub Ub Ub Ub
DA1
Ub Ub Ub Ub
DAR1
Ub Ub Ub Ub
DAR2

UBP15   TCP15   TCP22
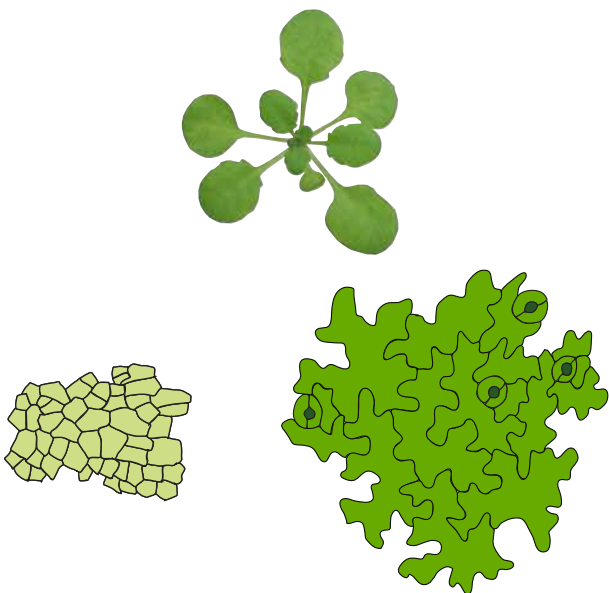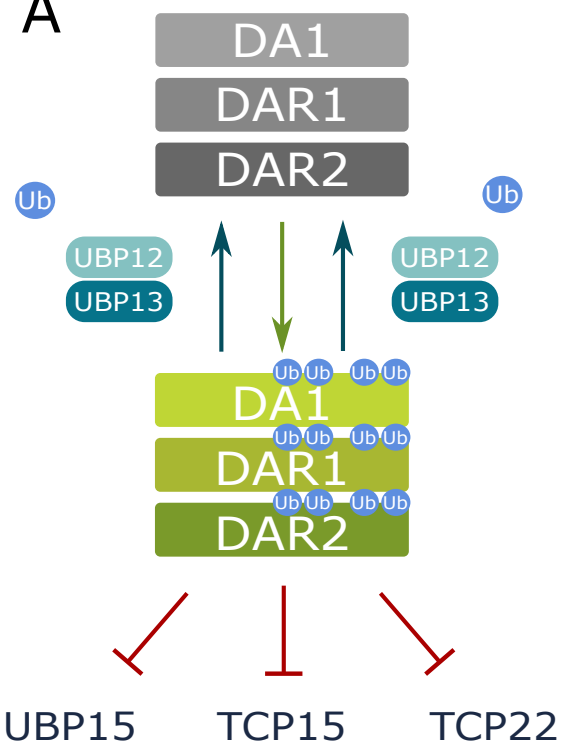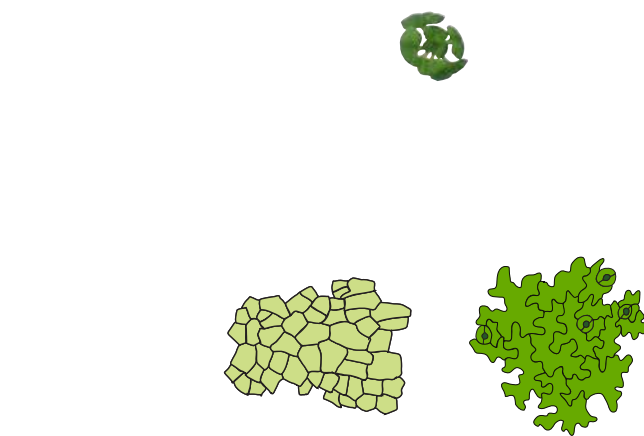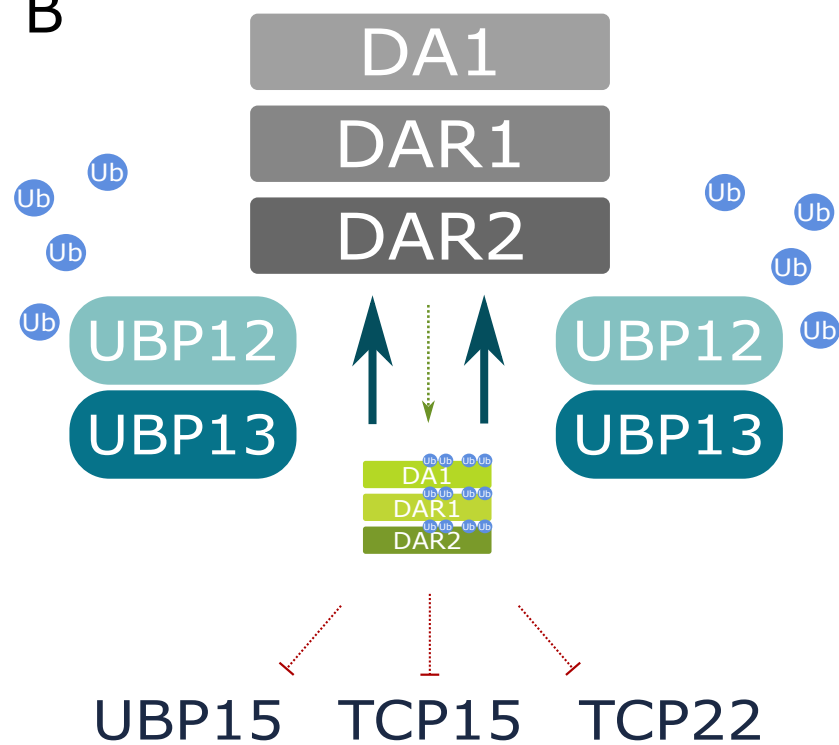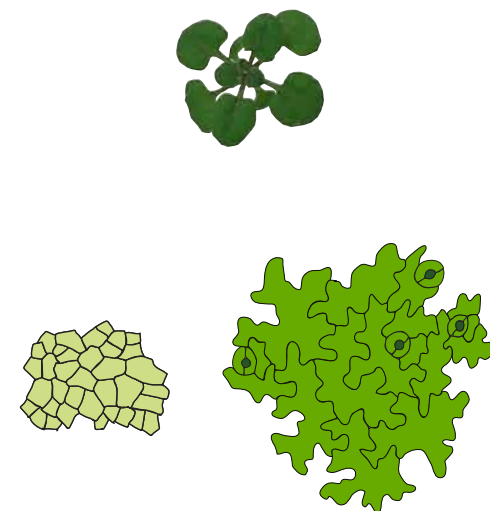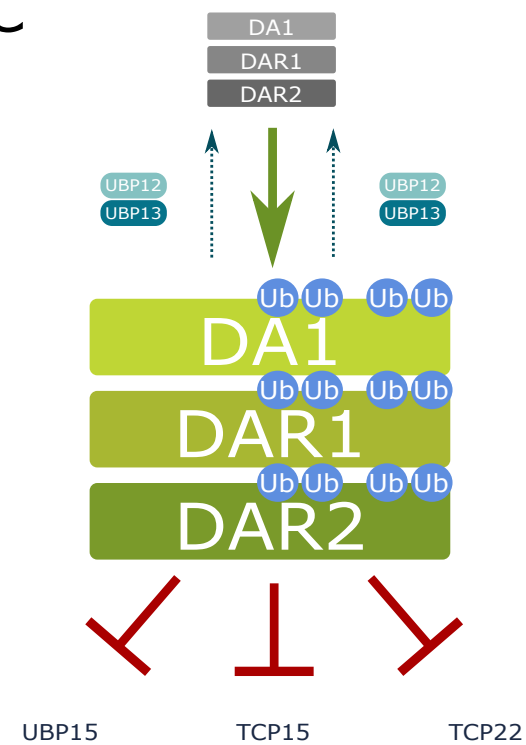
→ Activation   ⊣ Cleavage   → De-ubiquitination
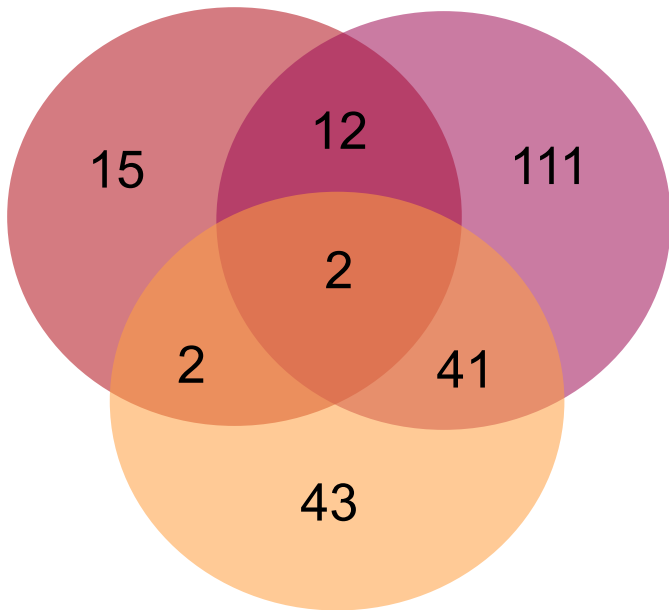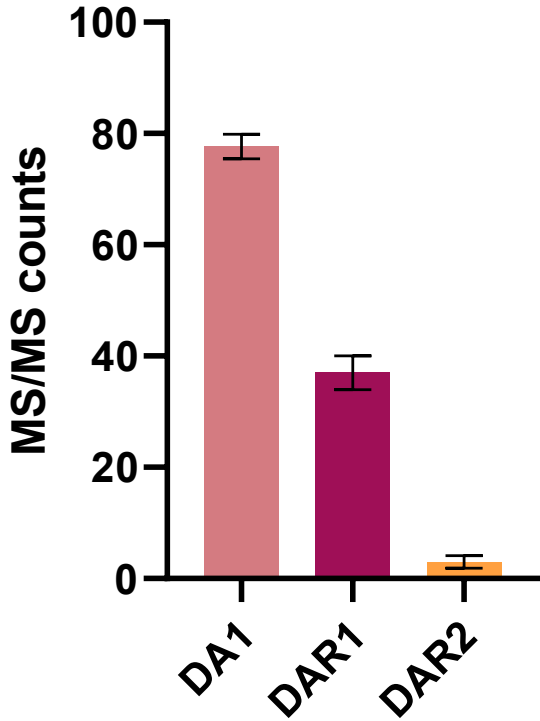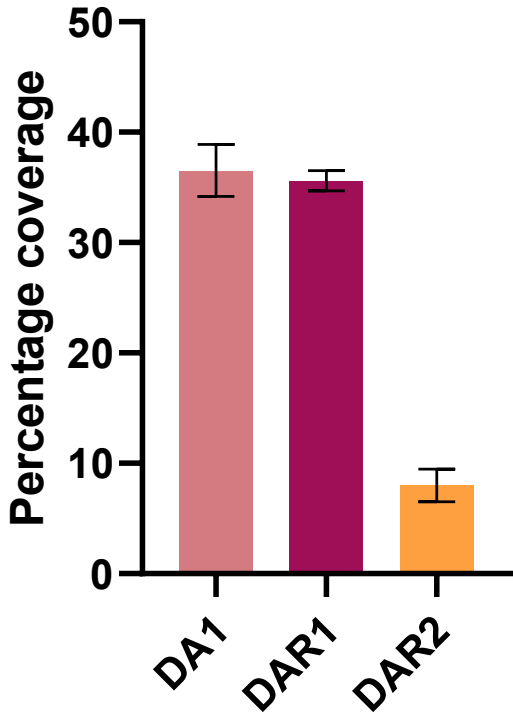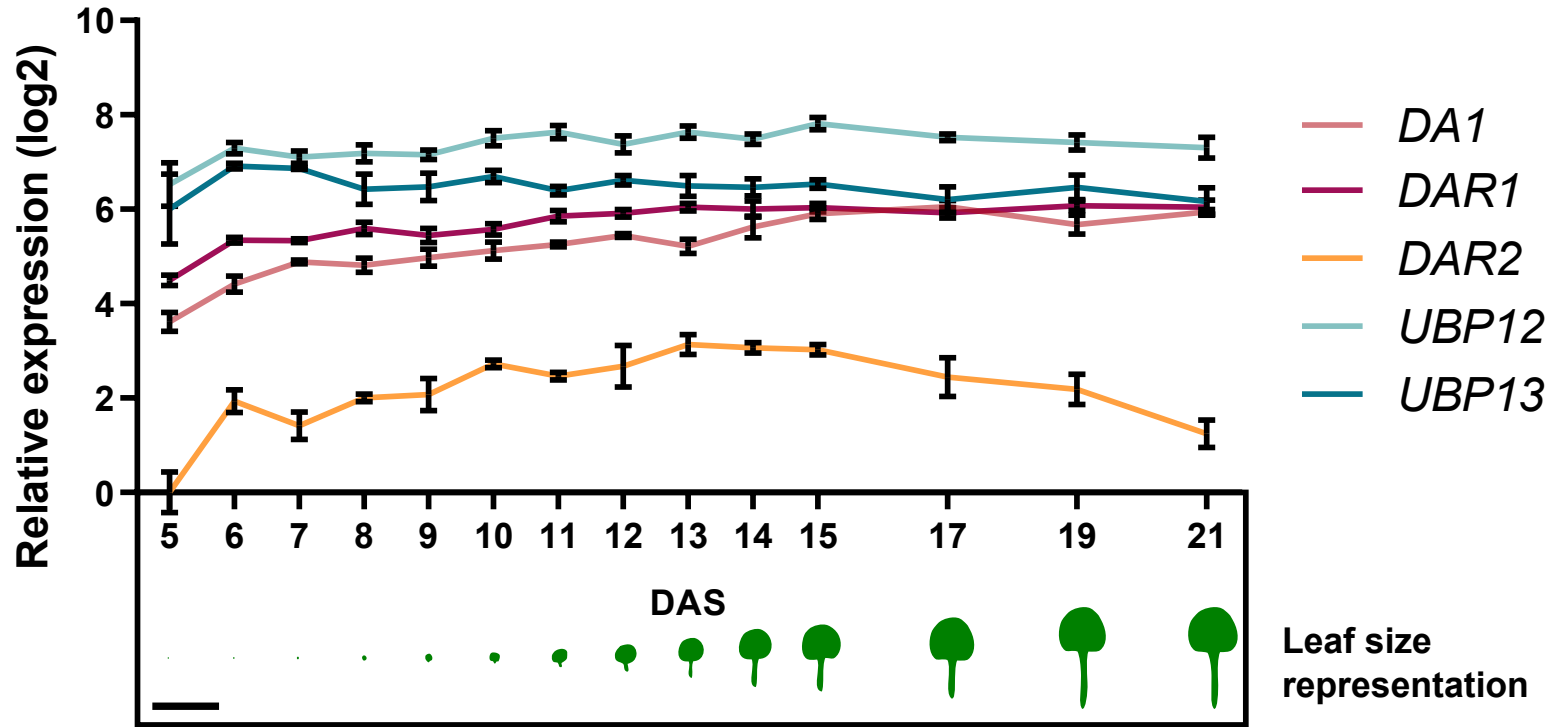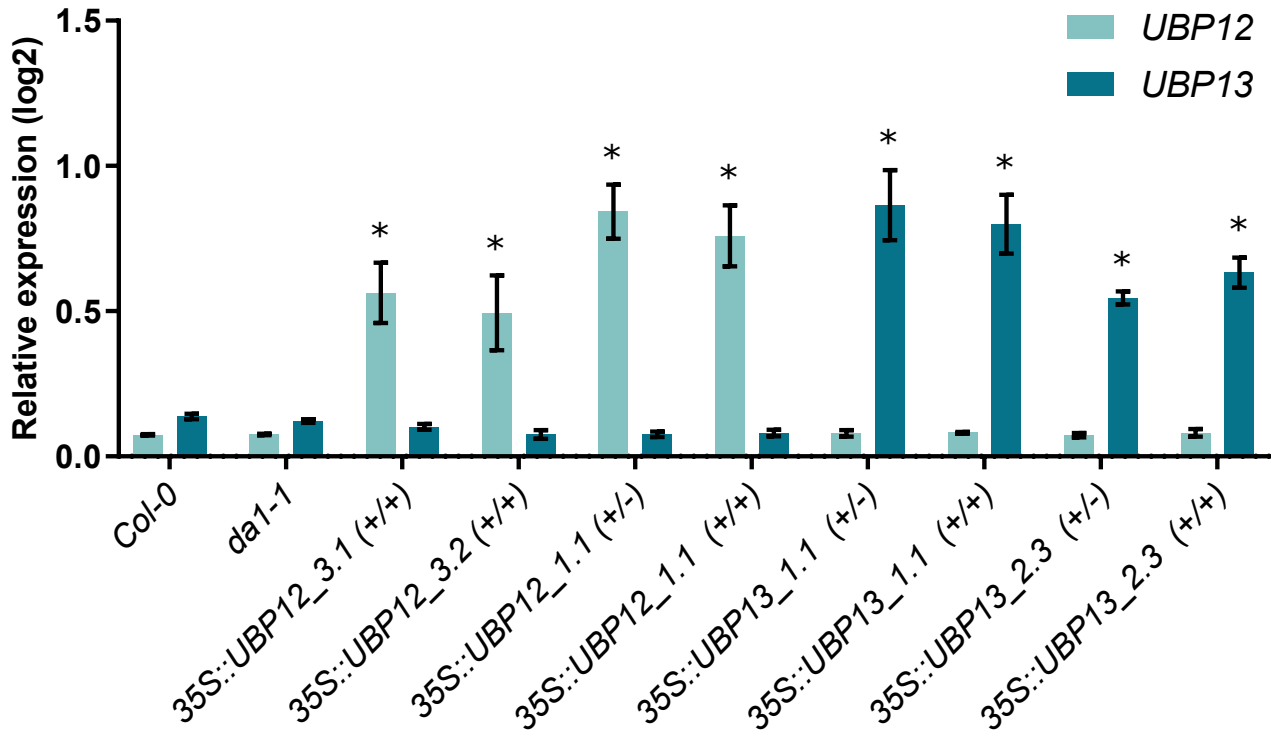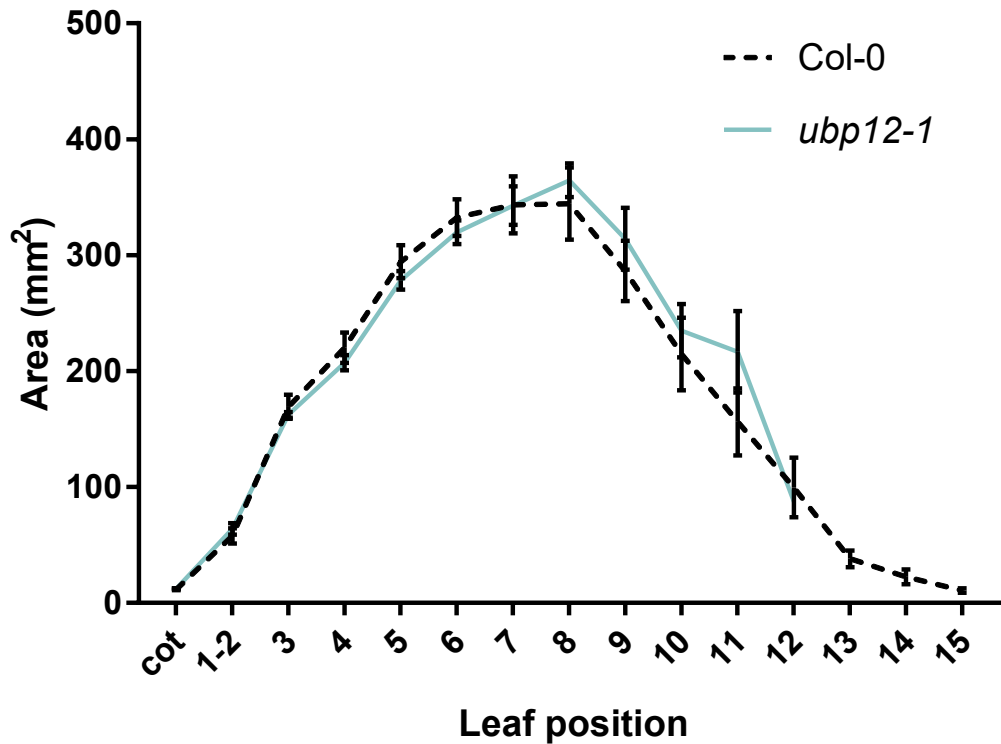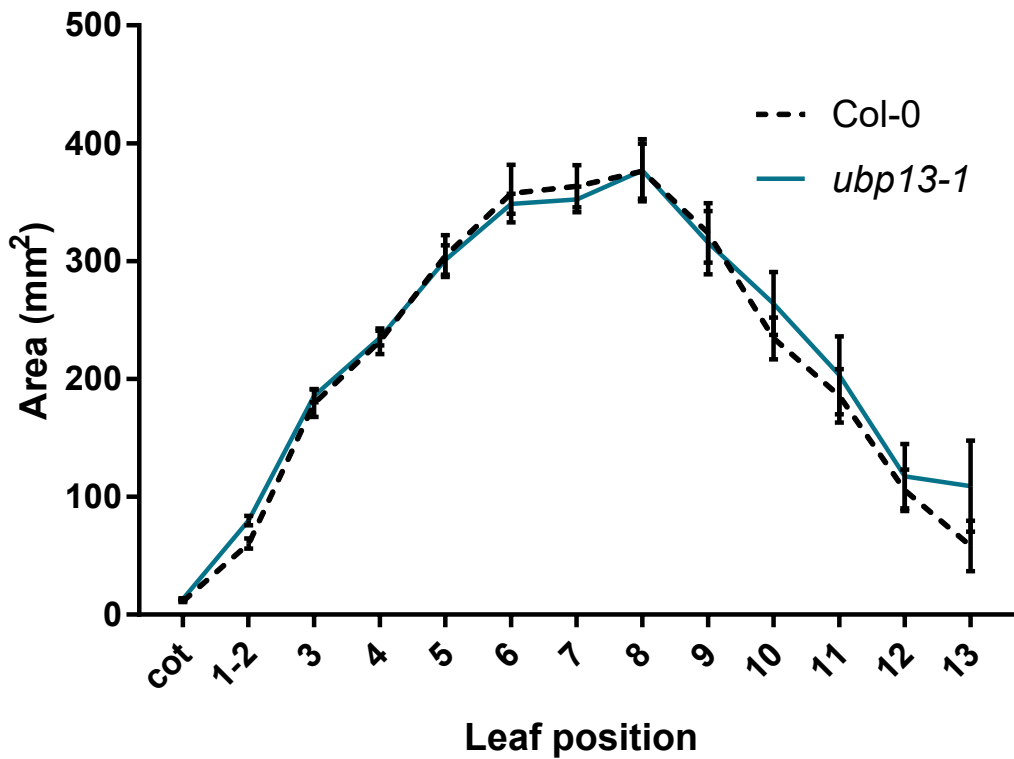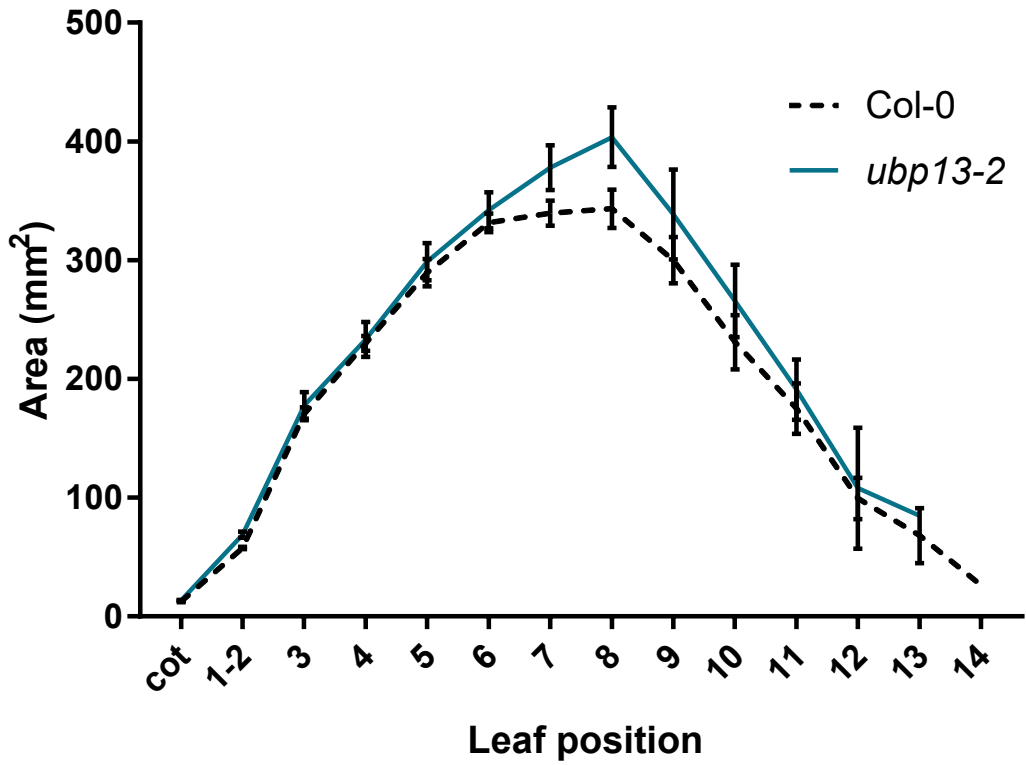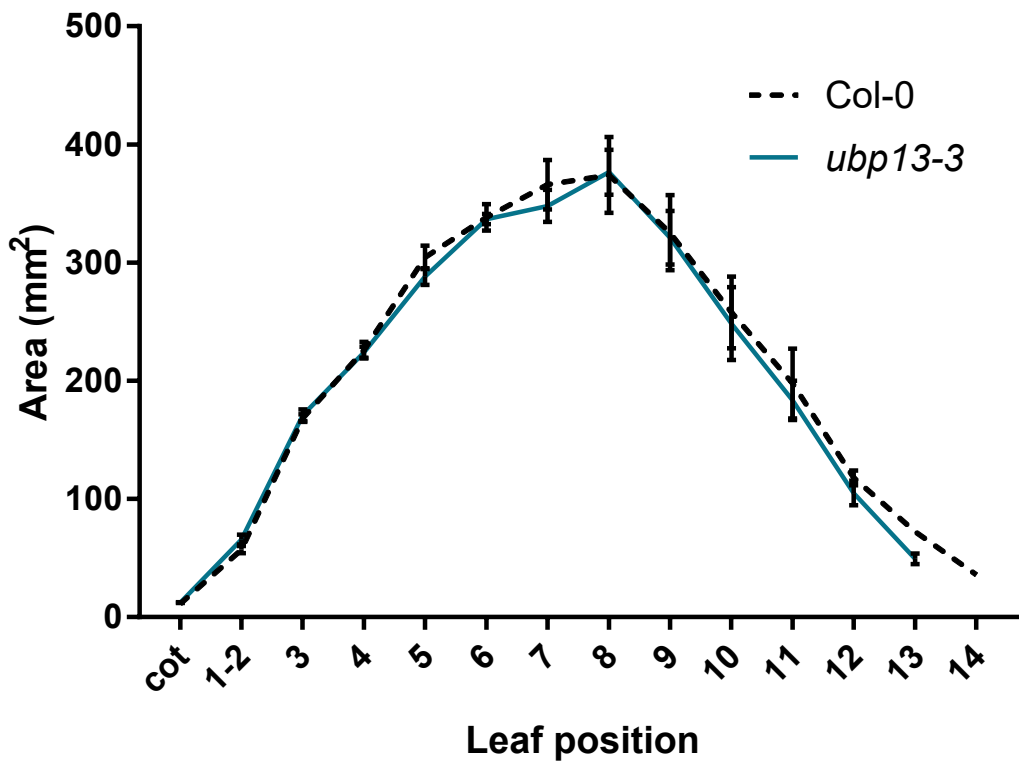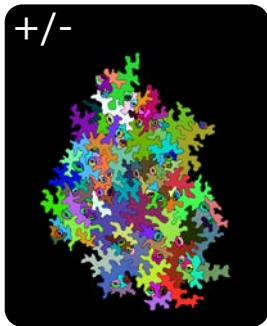
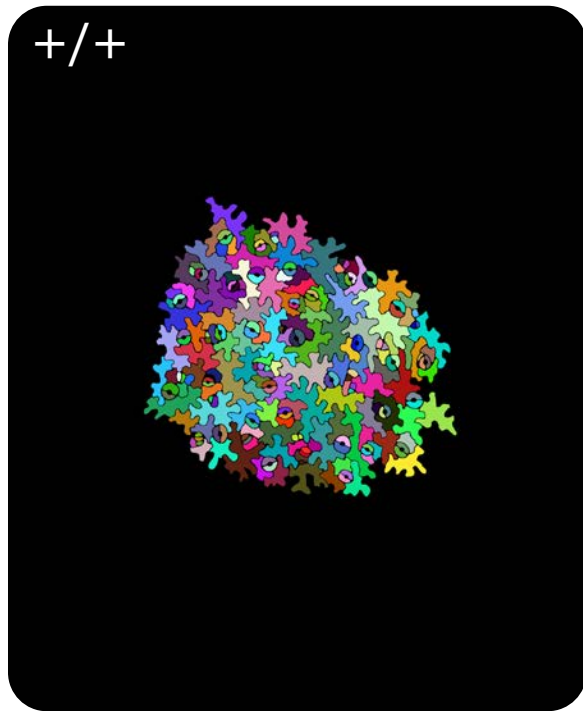| Col-0 | *35S::UBP12_3.1* | *35S::UBP12_3.2* |
| | +/- | +/- |

| Col-0 | *35S::UBP13_1.1* | *35S::UBP13_2.3* |
| | +/- | +/- |
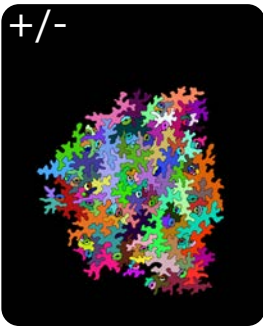
Col-0

35S::UBP13_1.1 (+/+)

+/+

Y-axis: Endoreduplication index

X-axis: Days after stratification

D9 D12 D15 D18 D21 D24 D27

Col-0

35S::UBP12_3.1

Day 15

Legend:
- *UBP12*
- *UBP13*
- *DA1*

Y-axis: Relative expression (log2)

X-axis categories:
- Col-0
- 35S::GFP-DA1
- 35S::UBP12_3.1 (+/-)
- 35S::UBP12_3.1 (+/+)
- 35S::UBP12_3.2 (+/-)
- 35S::UBP12_3.2 (+/+)
- 35S::UBP13_2.1 (+/+)
- 35S::UBP13_2.2 (+/-)
- 35S::UBP13_2.2 (+/+)

35S::GFP-DA1 background